KUNGL
TEKNISKA
HÖGSKOLAN

VETENSKAP
OCH
KONST

M.Sc Thesis

Simulation of neutron fluxes around the W7-X Stellarator

Jenny Andersson

Stockholm 1999

Department of Nuclear and Reactor Physics,
Royal Institute of Technology,
Stockholm, Sweden

MASTER OF SCIENCE THESIS

Examiner: Doc. Waclaw Gudowski
Supervisor: Dr. Thomas Elevant

Abstract

A new fusion experiment, the WENDELSTEIN 7-X Stellarator (W7-X), will be undertaken in Greifswald in Germany. Measurements of the neutron flux will provide information on fusion reaction rates and possibly also on ion temperatures as function of time. For this purpose moderating neutron counters will be designed, tested, calibrated and eventually used at W7-X.

Extensive Monte-Carlo simulations have been performed in order to select the most suitable detector and moderator combination with a flat response function and highest achievable efficiency. Different detector configurations with different moderating materials have been tried out, showing that a 32 cm thick graphite moderating BF_3-counter gives the desired flat response and sufficient efficiency.

Neutron spectra calculations have been made for different torus models and the influence of floor, walls and ceiling (i.e. reactor hall) have been investigated. Presented results suggest that a more detailed torus model significantly reduces the number of neutron counts at the detector. Calculations including the reactor hall indicate a tendency of shifting the neutron spectra towards the thermal region. The main part of the scattered neutrons are back-scattered from the floor.

Finally, calculations on the graphite moderating BF_3-counter in the detailed torus environment were performed in order to assess the absolute response function under the influence of the reactor hall. The results show that the detector count rate will increase by only 5-7 % when the reactor hall is taken into account. With a stellarator generating 10^{12} to 10^{16} neutrons per second the detector count rate will be $2 \cdot 10^5$ to $2 \cdot 10^9$ neutrons per second.

Contents

List of Figures

List of Tables

1   Introduction

A new fusion experiment, the WENDELSTEIN 7-X Stellarator (W7-X), will be built at the newly founded Max-Planck-Institute in Greifswald in Germany. In March 1996 the W7-X was approved by the European Commission. The investment costs (estimated to about 600 million DM) are put up by the European Union together with the Federal Ministry of Research and the State of Mecklenburg-Vorpommern [1]. The W7-X device is planned as the world's largest stellarator experiment with a major plasma radius of 5.5 meters and a magnetic field of 3 tesla [2]. It will use deuterium as fuel.

The stellarator is estimated to generate 10^{12} to 10^{16} neutrons per second depending on the heating scenario applied [3]. Measurements of the neutron production will provide information on fusion reaction rates and possibly also on ion temperatures as function of time. For this purpose moderating neutron counters will be designed, tested, calibrated and eventually used at W7-X.

The work presented in this report comprises Monte-Carlo calculations of neutron transport for fusion neutrons in moderating counters using MCNP Version 4B [4] with cross section data taken from ENDF/B-VI. The aim is to obtain a flat detector response function, that is to obtain equal sensitivities to neutrons with high (1-3 MeV) and low (>10 keV) energies. The purpose of this is to facilitate flux calibration by means of a neutron source with well known strength but with an energy spectrum significantly different from the fusion neutron spectrum. Effects from different geometric configurations and materials have been studied in the calculations.

Part of the work was performed at the Institut für Angewandte Physik, Universität Heidelberg in Heidelberg, Germany under supervision of Dr. Björn Wolle.

The thesis is divided into the following parts:

- Introduction to the Monte-Carlo method and description of specific features of MCNP [4] used.

- Monte-Carlo modeling of detector, torus and reactor hall geometries and modeling of fusion neutron sources.

- Neutron spectra calculations and comparison of different torus models with and without ports. Investigation of the influence of surrounding floor, walls and ceiling on the neutron spectra.

- Calculation of detector response function with mono-energetic neutrons, compared for different types of detectors and moderators.

- Determination of absolute detector efficiencies of the BF_3-counter for various BF_3-gas pressures. Calculation of detector efficiencies as function of moderator thickness, using different moderating materials and different neutron energy spectra in order to select the most suitable detector and moderator combination.

- Results from final calculations of the absolute response for a suitable detector with a torus model that best describes the real geometric configuration. Investigation of effects from floor, walls and ceiling in order to assess the magnitude of the absolute response.

- Important cross section plots and material compositions are shown in the Appendices. A brief introduction to neutron detection and controlled fusion is also given.

2 Monte-Carlo method

Methods of solving problems in physics can be classified as deterministic (i.e. solving differential equations) and statistical. The Monte-Carlo method is a statistical method originating from neutron diffusion problems but is nowadays applied to many problems in physics (particularly in particle transport calculations), mathematics and other sciences.

The most important difference between statistic and deterministic codes is that a statistic code creates a mean value of the particle behavior whereas a deterministic code solves the transport equation for the average particle.

Monte-Carlo methods are based on probability theory. The calculations are performed by random sampling from probability density functions describing the physical system. Examples of such functions are the different reaction cross sections of neutrons.

2.1 MCNP

This section will provide a short introduction of the basic principles in the Monte-Carlo Transport Code MCNP [4].

MCNP is a general code for calculating the time-dependent continuous-energy transport of neutrons, photons and/or electrons in three dimensional geometries. Both fixed source and criticality problems can be solved. The code is well suited to simulate complicated particle transport because it uses continuous cross section data. There are many powerful techniques to improve the efficiency of difficult calculations.

2.1.1 Geometry

MCNP treats an arbitrary three-dimensional configuration of materials in geometric cells. The cells are treated in a Cartesian coordinate system and are formed by intersections, unions, and complements of regions bounded by surfaces. MCNP handles first- and second-degree surfaces and fourth-degree elliptical tori. There is a number of tools to build complicated geometries, for example repeated structures. MCNP also provides a geometry-plotting capability which helps the user to check for geometry errors.

The material composition in each cell is specified by the isotopic composition.

2.1.2   Tallies

The result of a MCNP calculation is obtained by collecting the outcome from many simulations (tallying). Results can be obtained as currents, fluxes, energy deposition, detector responses and reaction rates. These are averaged either over a surface or over a cell. All tallies are normalized per source particle except in criticality problems.

2.1.3   Error estimation and variance reduction

Extensive statistical analysis of a simulation is provided by MCNP. Ten statistical checks are made for each tally. It is important to note that the error estimations refer only to the precision of the MCNP calculation itself and not to the accuracy of the result compared to the true physical value.

There are many advanced techniques to reduce the statistical error (variance) and to improve the efficiency of a calculation implemented in the code. They are all based on the principle that particle histories which contribute to the result should be sampled in favor of histories that do not contribute as much.

2.1.4   Cross sections

MCNP uses pointwise (continuous) cross section data from evaluated nuclear data libraries (like ENDF/B-VI, JEF or JENDL). These data libraries use sophisticated methods to create pointwise cross section data files based on experimental results in combination with theoretical models. The data files contain probabilities for cross sections, angular distribution etc governing the sampling. The reliability of MCNP is based on the accuracy of these data. The cross section libraries for neutron-reactions are isotope specific, whereas electron- and photon-reactions are atom specific. Besides neutron-, electron- and photon-reaction cross sections there are also so called neutron thermal $S(\alpha, \beta)$ tables, which are essential to give correct answers in analyses involving neutron thermalization. The $S(\alpha, \beta)$-model accounts for the up- and down-scatter (i.e

gaining or loosing energy) of neutrons when interacting with other parti-
cles at thermal energies (below about 4 eV). This is an effect of chemical
binding and crystal structure. The S(α, β) capability is available for a
limited number of substances and temperatures.

3 Modeling the problem

The problem is set up in two different parts:

- Stellarators and reactor hall

- Detectors and moderators

The two parts are modeled separately and calculations are also performed separately for each part. Finally, they are combined and some special features are calculated for the complete set up. Two different types of neutron sources are used. First, a fusion line source is modeled, and used in all the calculations with the stellarators involved. Second, an isotropical surface source placed on the detector or moderator surface is used when essential properties of the detectors are studied.

The geometric configurations and some special features of MCNP used are described below. Important cross sections are plotted in Appendix A, and material compositions and cross sections used are specified in Appendix B.

3.1 Fusion neutron source and geometry

This section describes the fusion neutron source. It is modeled in the same manner for different stellarator models. When calculations are made with a detector, the fusion source is located on the symmetry axis in the center of the torus.

Two different types of tori are modeled. One quite non-sophisticated torus consisting only of a vacuum vessel (called the Simple model) with and without ports[1] and a model with ports, describing the real geometry of the W7-X stellarator in more detail. The latter is referred to as the W7-X model. The W7-X torus is a modified version of a model of the WENDELSTEIN 7-AS stellarator[2], which was modeled in MCNP by G. Beikert[3]. It includes real material data of W7-AS, although the

---

[1] A port is a window between the outside of the stellarator and the plasma. Different diagnostic equipments are placed by the ports in order to investigate the plasma, radiation emitted etc.

[2] W7-AS is a fusion experiment located at the Max-Planck-Institute für Plasmaphysik in Garching, Germany. The stellarator has a major plasma radius of 2 m and a mean minor plasma radius of 0.2 m [5].

[3] Institut für Angewandte Physik, Universität Heidelberg, Heidelberg, Germany.

magnetic coils, support structure and cladding materials are treated as a homogeneous mixture. The modification of the W7-AS torus to the W7-X torus is made by enlarging the dimensions to those of W7-X. Ten inward horizontal ports are also added.

This section also provides a description of the the reactor hall. No experimental equipment or other devices in the reactor hall are considered in the calculations. The stellarator is surrounded only by concrete floor, walls and ceiling.

All the material compositions, densities and cross sections used are specified in Tables 3, 4, 5, 6 and 7 in Appendix A.

3.1.1   Fusion neutron source

The fusion neutron source has a Gaussian energy spectrum. In MCNP this is modeled with a built-in analytic function which generates a continuous probability density function for the source variable [4]. The energy distribution is given by:

$$p\,(\,E_n\,)\;=\;C_1\;\exp\big[\,-\,(\,\frac{E_n\,-\,\langle\,E_n\,\rangle}{C_2\,T\,\langle\,E_n\,\rangle}\,)^{\,2}\,\big]$$

where

$$
\begin{aligned}
\langle\,E_n\,\rangle \;&=\; \text{average neutron energy in MeV}\\
T \;&=\; \text{plasma temperature in MeV}\\
C_1,\;C_2 \;&=\; \text{constants}
\end{aligned}
$$

Since D-D fusion is considered the mean energy of the emitted neutrons is 2.45 MeV. The plasma temperature is estimated to be about 3 keV in the W7-X stellarator, and the corresponding neutron energy spectrum is shown in Figure 1.

The geometric extent of the source is modeled as a circular line source, with zero radial extension, going through the center of the stellarator vacuum vessel. This is shown in Figures 2 and 3. The neutrons are emitted isotropically.

In order to shorten the calculation times for the detector efficiency calculations as function of the moderator thickness for different detector and torus configurations, a feature where MCNP writes a new source
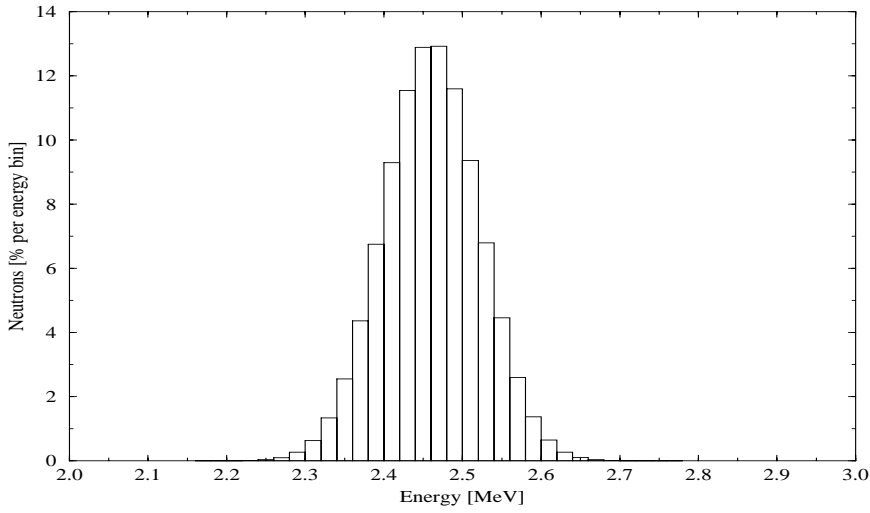
Figure 1: *D-D fusion neutron energy spectrum for a plasma temperature of 3 keV, plotted by MCNP version 4B. The distribution is given in per cent of neutrons per energy bin as function of energy.*

from the original one is used. A new source is created on an artificial surface around the detector. This source contains only those neutrons from the original fusion source that have reached the detector area. The source can be used over and over again while the detector properties are changed. This of course saves a lot of time since the neutrons not going in the direction of the detector only have to be followed once.

3.1.2   Simple torus model

The Simple torus model is composed only of a 0.1 m thick stainless steel vacuum vessel. It has a major plasma radius of 6 m. The poloidal cross section is circular, with a minor inner radius of 0.7 m. This model is created with and without 10 ports, equally spaced around the torus on the horizontal mid-plane of the torus pointing inwards. The ports are cylindrical holes through the vacuum vessel, with a radius of 12 cm. The geometric configuration of the model is shown in Figure 2.

3.1.3   W7-X torus model

The W7-X model also has a major plasma radius of 6 m. The poloidal cross section is oval-shaped, with a mean minor inner radius of 1 m. The torus consists of an inner, 0.012 m thick, stainless steel vacuum vessel and an outer stainless steel containment vessel with a mean thickness of 0.037 m. The stainless steels of the vacuum vessel and containment vessel, used in the calculations, have very high densities[4]. These densities correspond to an increase in the thicknesses of the vessel walls of about three times compared to if the true densities of the steels would have been used. Between the two vessels is a homogeneous mixture of materials, composed mainly of copper and nickel, and with a mean thickness of 0.7 m. This represents magnetic coils, support structure and cladding materials. Ten ports are equally spaced around the torus, located on the horizontal mid-plane pointing inwards. The ports are cylindrical holes through all the vessels, with a radius of 0.12 m. The complete geometry is shown in Figures 3 and 4.

Calculations making use of the W7-X model involve very long neutron transport through a lot of material. In order to get acceptable statistics within a reasonable time, some variance reduction techniques have been used. In all the calculations with the W7-X torus, a DXTRAN sphere is used around the detector region. DXTRAN is used to improve the particle sample in the vicinity of a tally. It is typically used when a small region is being inadequately sampled because particles have a very small probability of scattering toward that region. When floor, walls and ceiling are added to the model, the neutron importances in the different MCNP cells are also changed. An increased importance will help particles move to more important regions of the geometry. If neutrons head in an unfavorable direction, they are killed. These variance reduction techniques are described in detail in [4].

3.1.4   Reactor hall model

The reactor hall is modeled as a rectangular room made of 0.4 m thick concrete floor, walls and ceiling. The shortest perpendicular distance from each wall and the ceiling to an outer surface of the torus is 10 m. The floor is 0.5 m below the bottom surface of the stellarator. This

---

[4]This does not simplify the Monte-Carlo calculations but the W7-AS was modeled in this way by G. Beikert (see 3.1) for other reasons.

causes the hall to be slightly larger in the W7-X model than in the case of the Simple model, since the W7-X torus has a greater minor plasma diameter. The geometry of the reactor hall is shown in Figure 5.

Neutron spectra and detector count rates are calculated with the floor only and with the complete hall to evaluate the difference. The real floor, walls and ceiling are supposed to be about 1.5 m to 2 m thick, depending on what kind of concrete will be used[5]. Together with the Simple model a 1 m thick floor is used to calculate its influence. Thicknesses of more than 0.4 m gives a contribution to the detector count rate that is less than the statistical errors in the calculations. Using only 0.4 m of concrete therefore gives adequate accuracy and saves a lot of calculation time.

---

[5] If the concrete contains boron, which has a very large neutron absorption cross section, less concrete is needed for sufficient neutron shielding.

1. Circular line source
2. Vacuum vessel
3. Vacuum
4. 10 horizontal ports

Scale 1:220
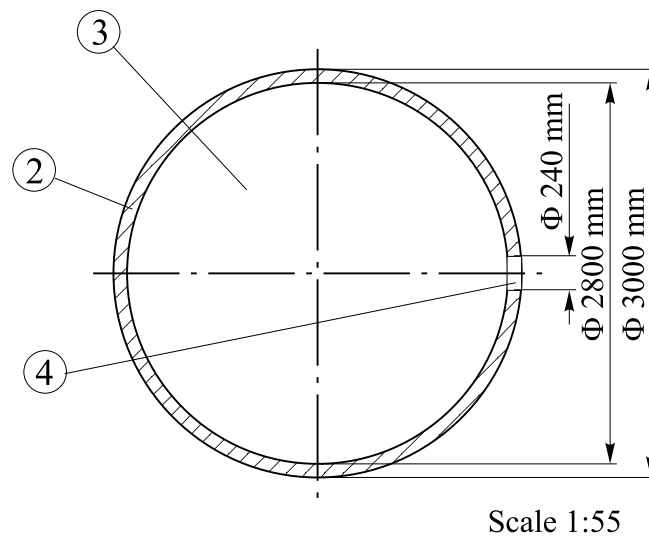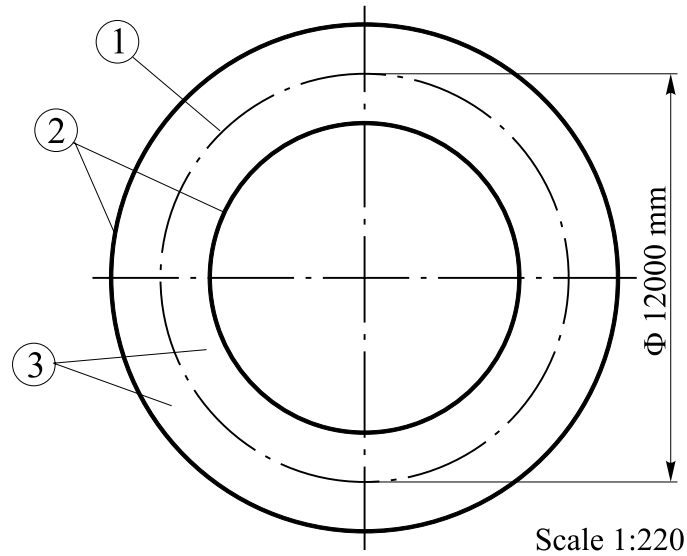
Scale 1:55

Figure 2: *The Simple torus model with ports. Top: toroidal cross section in scale 1:220. There are 10 horizontal ports which are to small to be shown in the figure. Bottom: Poloidal cross section in scale 1:55.*

1. 10 horizontal ports
2. Containment vessel
3. Vacuum vessel
4. Circular line source
5. Vacuum
6. Coils and support structure
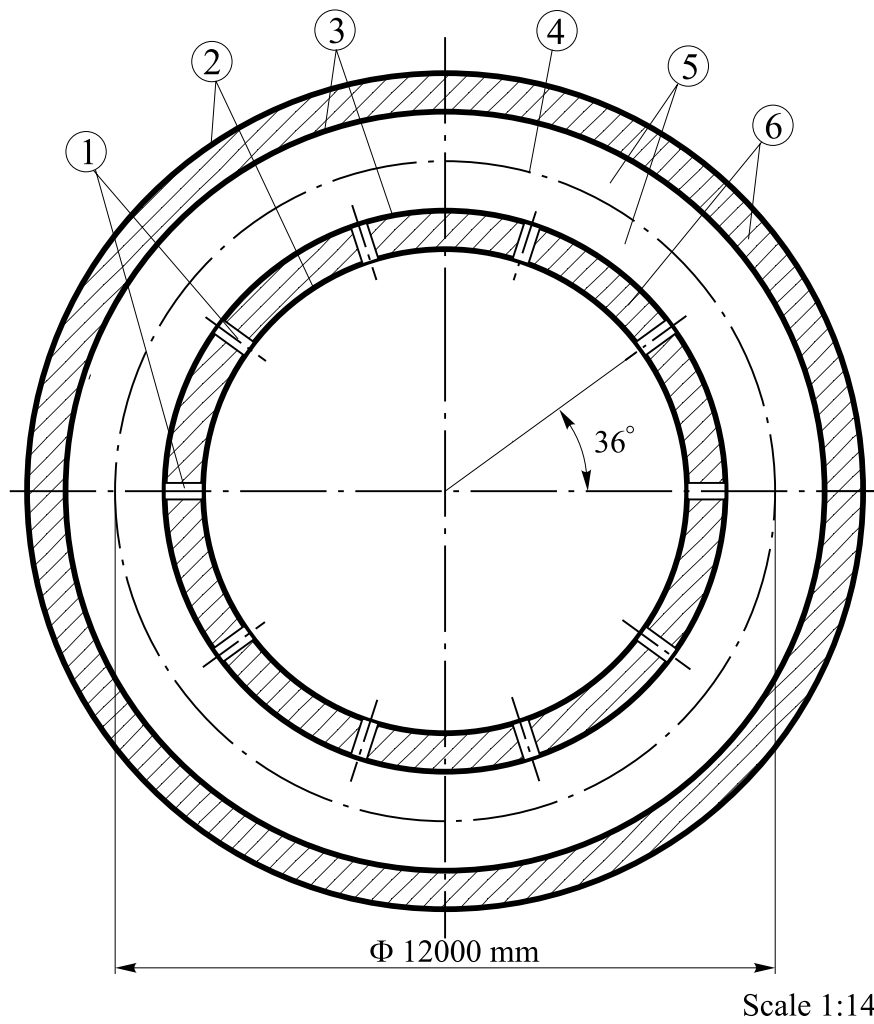
Figure 3: *Toroidal cross section of the W7-X torus model in scale 1:140.*

1. Vacuum
2. Vacuum vessel
3. Coils and support structure

4. Containment vessel
5. 10 horizontal ports
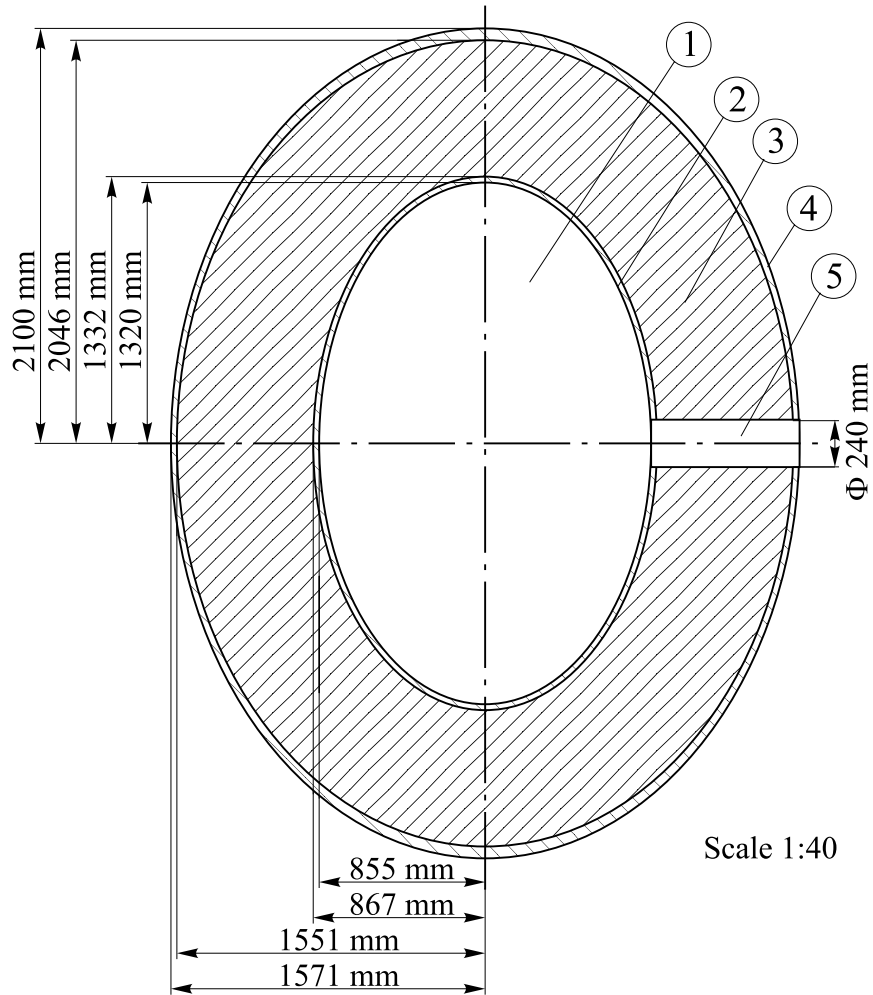
Figure 4: *Poloidal cross section of the W7-X torus model in scale 1:40. The source runs through the center of the vacuum vessel.*
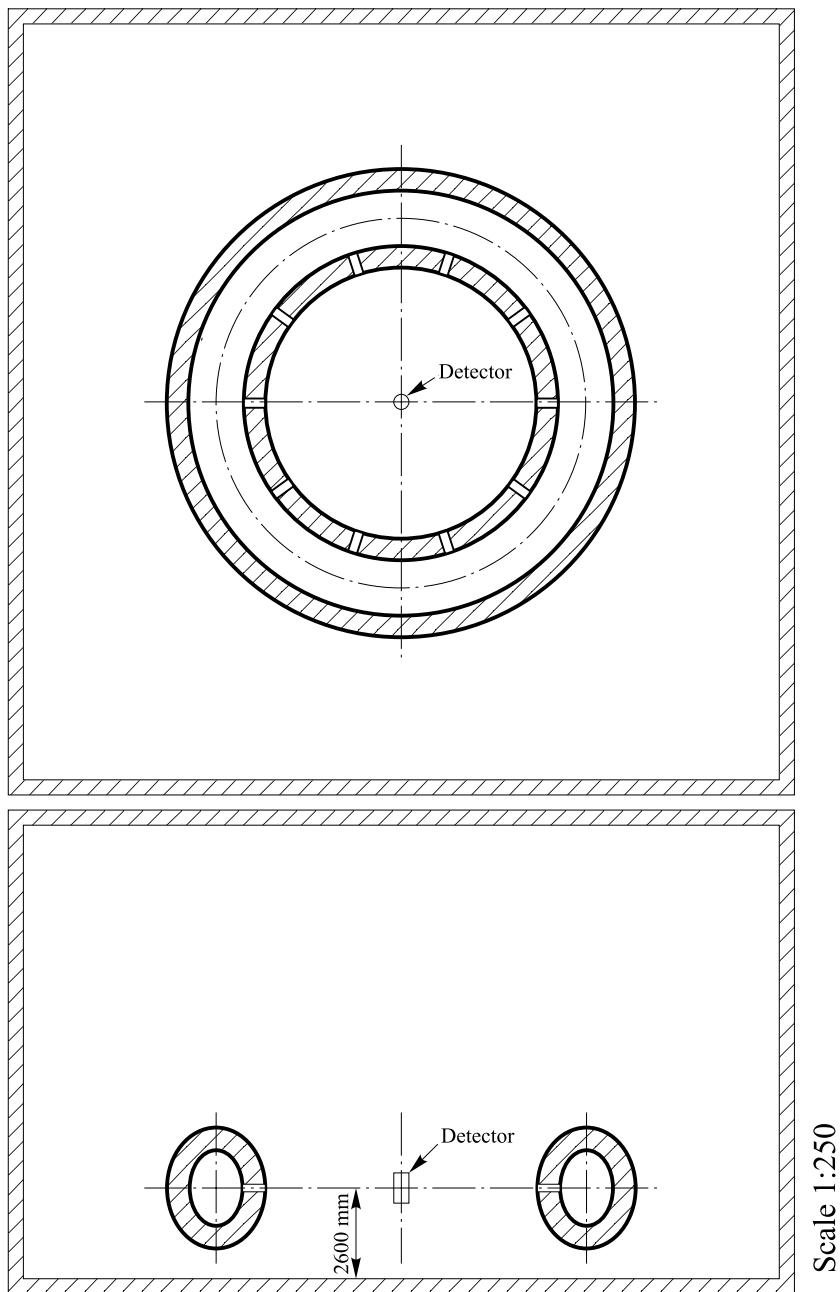
Figure 5: *Cross sectional top and side view of the reactor hall with the W7-X torus in scale 1:250. The distance between floor and symmetry axis is 2000 mm when the Simple torus model instead is considered.*

3.2   Detectors, moderators and surface sources

Three different types of detectors are modeled: BF$_3$-counters, thermal fission chambers and fast fission chambers. The different material compositions of the detectors and moderators, their densities and cross sections used in the calculations are specified in Tables 8, 9 and 10 in Appendix B.

3.2.1   Neutron detectors

Cylindrical detectors are modeled as 200 mm long cylinders with a diameter of 35 mm, as shown in Figure 6. The BF$_3$-counters contain BF$_3$-gas at 1 atm pressure, and density $\rho = 0.002735$ g/cm^3. The boron is pure ^{10}B with atomic density $a = 2.43 \cdot 10^{-5}$ atoms/cm·barn. Both types of fission chambers are coated with a 0.6 μm thick layer of a fissile isotope on the inside of the cylindrical surface. This corresponds to 250 mg ^{235}U. Calculations are performed with the isotopes ^{235}U or ^{239}Pu for thermal fission chambers. The isotopes ^{238}U or ^{237}Np are used in fast fission chambers.

(a) BF_3-counter

(b) Fission chamber
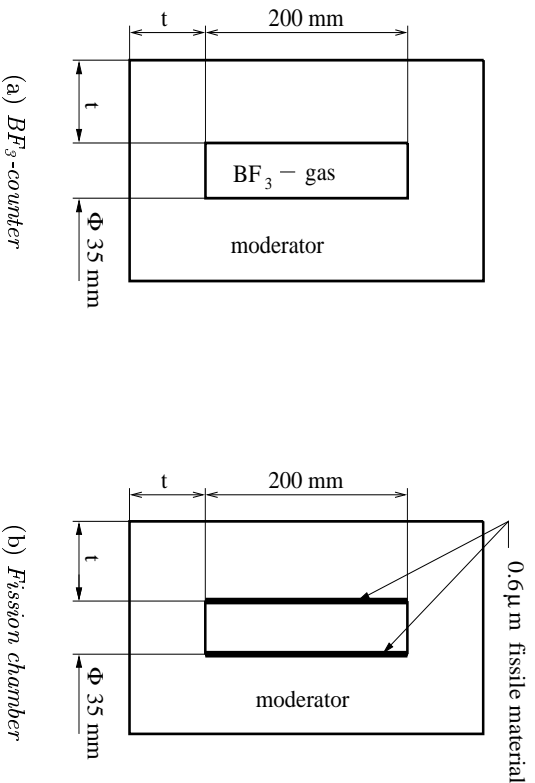
Figure 6: Cylindrical detector geometry

For simplicity, spherical BF$_3$-counters (as shown in Figure 7) with a diameter of 100 mm are used when the detector efficiencies as function

of moderator thickness for direct fusion neutrons are calculated. The composition of the BF$_3$-gas filling the detector is equal to that of the cylindrical BF$_3$-counter described above.
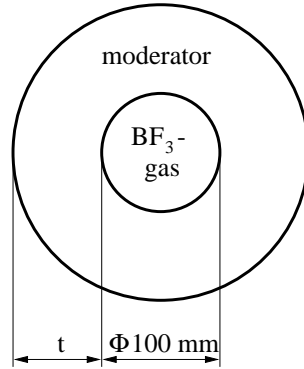
Figure 7: *Spherical detector geometry*

3.2.2   Moderators

Since direct fusion neutrons are fast (i.e. 2.45 MeV) they have to be slowed down in order to be efficiently detected in BF$_3$-counters or thermal fission chambers. For this purpose the detector is surrounded by a cylindrical moderator shell. In Figures 6 and 7 the different detector designs are shown. The moderator has the same thickness t on the top and on the bottom of the cylinder as on the cylindrical surface. For fast fission chambers t is equal to zero.

The detector efficiency is calculated as function of moderator thickness for direct fusion neutrons. Results with various conventional moderator materials like water, heavy water, beryllium, graphite and polyethylene are compared. For neutron spectra and detector response function calculations, polyethylene and graphite are chosen for practical purposes and because they behave quite different as moderators.

Thermal S(α, β) cross sections (described in Section 2.1.4) are used for the moderating materials to get an accurate treatment of elastic and inelastic scattering during neutron thermalization.

3.2.3   Detector surface source

Two different neutron sources are modeled. First, when calculating the detector response function, an isotropic cylindrical surface source emitting mono-energetic neutrons is used. Second, when calculating the detector efficiency as function of moderator thickness for direct fusion neutrons, mono-energetic neutrons are substituted by the MCNP built in function for Gaussian fusion energy spectrum, see Section 3.1.1.

For the BF_3-counters and thermal fission chambers the source is located on the outer surface of the moderator. In the case of fast fission chambers the source is located directly on the detector surface. As illustrated in Figure 8a for the cylindrical detectors, this means that about 50 % of the neutrons are incident on the moderator/detector surface and 50 % are lost in the outward direction. It may seem unnecessary to loose particles in the outward direction but this is because the source is actually modeled in MCNP as an infinite small volume source and not as a surface source. In this case it is not possible to choose a surface-normal for the in- or outward directions. The spherical surface source however is modeled as a real surface source and it is thus possible to choose a surface-normal such that all neutrons are directed inward as shown in Figure 8b.

(a) *Cylindrical surface source*

(b) *Spherical surface source*
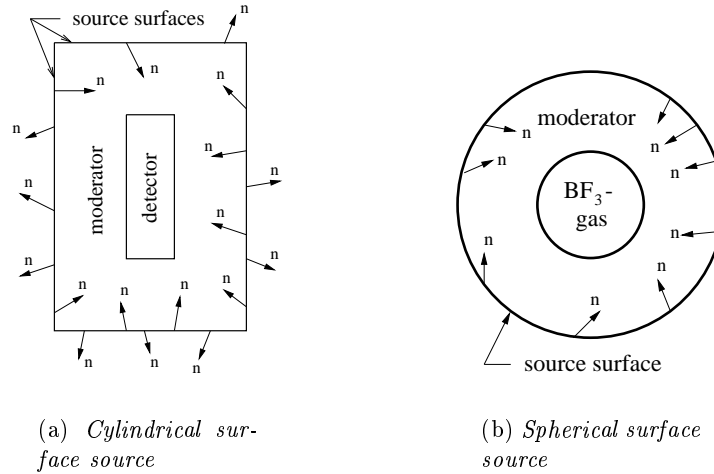
Figure 8: *Isotropical neutron sources located on the moderator surface.*

4 Torus calculations

In this section is the minimum thickness of floor, walls and ceiling necessary to obtain adequate accuracy in the calculations with the reactor hall determined. Neutron spectra for the two torus models are then calculated and compared for the tori alone and together with the floor. The number of neutrons per source neutron are counted on a cylindrical surface with radius 21.75 cm and height 30 cm (corresponding to a detector with a 20 cm thick moderator), placed at the detector position. For calculations of neutron energy spectra five energy bins, equally spaced in logarithmic scale, are used per decade.

4.1 Determination of concrete thickness

These calculations are carried out for the Simple torus model with ports and a 100 cm thick concrete floor. The Simple torus model with floor represents the worst case because the neutrons are not escaping the torus just through the ports but are also scattered through the vacuum vessel, as will be shown in Section 4.2. The floor is the part of the reactor hall that has the largest influence since it is closest to the detector.

The floor is divided into 10 cm thick segments. The number of neutrons that have entered a segment or passed beyond it, giving a detector contribution are counted. The results are shown in Table 1. It can be

segment	% of total counts
0-10 cm	42
10-20 cm	5.5
20-30 cm	0.8
30-40 cm	0.09
40-50 cm	0.0001
50-60 cm	0
60-70 cm	0
70-80 cm	0
80-90 cm	0
90-100 cm	0

Table 1: *Number of neutrons penetrating behind a certain segment of concrete before reaching the detector, given in % of the total number of neutrons at the detector for the Simple torus model with ports and floor.*

seen that 42 % of all the neutrons scoring at the detector have been scattered in the floor. This is a substantial amount of the neutrons, thus showing that scattering of the neutrons in equipment, floor etc will give an essential contribution to the count rate. However, only 0.09 % of the total number of neutrons reaching the detector have penetrated through more than 40 cm of concrete. It is only about 1/10 of the relative error in the calculation of the total number of detector counts. This concludes that having 40 cm of concrete wall thickness is more than sufficient to accurately estimate the influence of the reactor hall.

4.2   Neutron energy spectra

The calculations below are carried out with the Simple torus model including ports. A spectrum without ports is also calculated, resulting in a 17 % decrease of the 2.45 MeV fusion neutrons, compared to the spectrum with ports.

Neutron spectra from the two torus models with and without floor are shown in Figure 9. There is a noticeable difference between the two
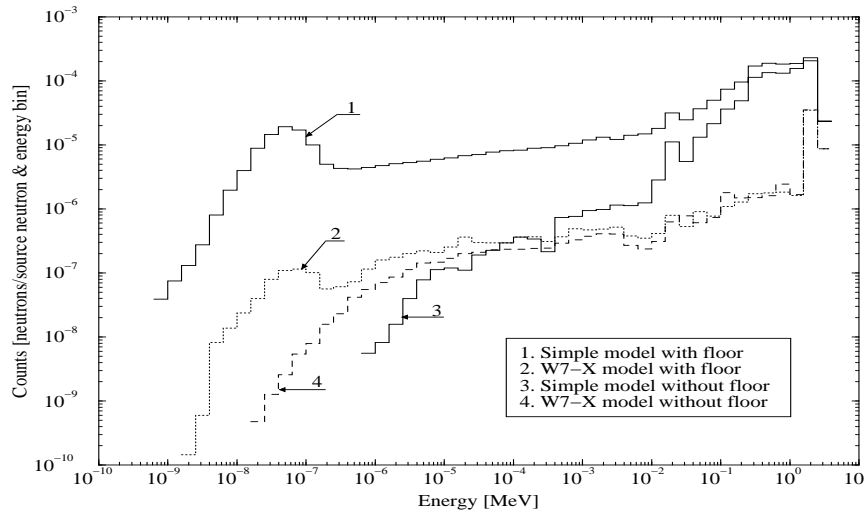
Figure 9: *Neutron spectra of the two torus models with and without floor given as the number of neutrons per source neutron and energy bin at the detector position and as function of energy. There are 5 energy bins per decade.*

models, resulting from the fact that for the Simple model the neutrons are scattered through the vacuum vessel and when there is no floor there are basically no thermal neutrons. When the floor is added a significant part of the neutrons are scattered in the concrete (i.e. 42 % for the Simple model as shown in Section 4.1). There is a very distinct peak of thermal neutrons. In the W7-X model most of the neutrons are fast fission neutrons because in principle all neutrons scoring at the detector passed through the ports, which are directed towards the detector. When the floor is added, there is again a peak in the thermal region of the spectrum. The almost linear decrease in the spectrum for the Simple torus model at higher energies is due to neutrons escaping through the vacuum vessel and they do not loose very much energy when scattered by iron. This implies that, if there will be a lot of steel equipment in the reactor hall blocking the ports, the true spectrum from W7-X might look more like the spectrum of the Simple model.

In Figure 10 is the spectrum of the W7-X model with the complete reactor hall shown together with other spectra of the W7-X torus. The
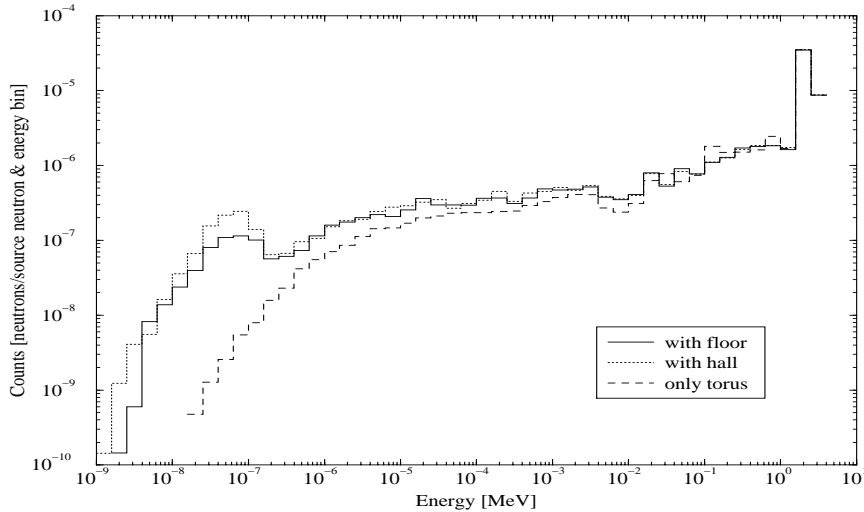
Figure 10: *Neutron spectra of the W7-X torus alone, with the floor and with the reactor hall (i.e. floor, walls and ceiling) given as the number of neutrons per source neutron and energy bin at the detector position and as function of energy. There are 5 energy bins per decade.*

small increase of neutrons in the thermal region lies within the uncertainties. Only a small increase is expected since the walls and the ceiling are very far away from the detector compared to the floor. The most essential issue will probably be whether there is going to be a lot of equipment that may cause neutron scatter.

5   Detector response function

The detector response function is a detector's sensitivity to mono-energetic neutrons as function of neutron energy. In this work, it is presented as the simulated reaction rate in the detector as function of the incident neutron energy. Mono-energetic neutrons are incident on the moderator surface when a moderator is used, and directly on the detector surface when there is no moderator. In order to facilitate yield calibration at the W7-X experiment the aim is to obtain a detector with equal sensitivity to fast and thermal neutrons, a so called flat response function. The most important region, is between 1 keV and 3 MeV.

In order to choose a good detector, certain contributory factors have to be considered when comparing the reaction rates for different moderator thicknesses because they are dependent on the neutron field. The calculations described below can be exactly compared only if the neutron field is homogeneous. That is the probability for neutrons to reach the moderator surface should be the same for any moderator size. In the response function calculations this is true because the neutrons are always started on the moderator surface. But, as will be shown in the efficiency calculations (see Section 6), the field simulating the reality is dependent on the distance from the source. This implies that the larger the moderator is, the closer it comes to the source and the greater is the detection probability. Once the neutron has reached the moderator there is always a probability to score in the detector. As long as the probability for this is larger than the probability for absorption in the moderator, a larger moderator is always preferred.

In the presented results the moderator thicknesses are given as the absolute thickness of the moderator, as shown in Figure 6 in Section 3.2. Only one example of an error bar is shown for each curve.

5.1   BF$_3$-counters

Detector response functions of a BF$_3$-counter for various polyethylene moderator thicknesses are shown in Figure 11. For the bare core detector (no moderator) the reaction rate drops quickly at high energies as expected from the (n,α) reaction cross section of ^{10}B (see Figure 24 in Appendix A). For increased moderator thicknesses more neutrons are thermalized and at the same time more of the initially low energy neu-

trons are lost through absorption and out scatter from the moderator. The maximum reaction rate moves towards higher energies as the moderator thickness is increased. At 4 cm a reasonable flat response function is obtained from 10 eV to 1 MeV but unfortunately 4 cm of moderator is not sufficient to slow down enough neutrons with 2.45 MeV energy.

Figure 11: *(n,α) reaction rates of polyethylene moderating BF₃ as function of incident neutron energy for different moderator thicknesses given in cm. The average relative error in the calculations is about 1.5 %. The lower picture shows only a few of the response curves in order to get a better separation in the high energy interval.*

Detector response functions of a BF$_3$-counter with graphite moderators of different thicknesses is shown in Figure 12.   Since graphite has a smaller elastic scattering cross section than polyethylene (see Figure 29

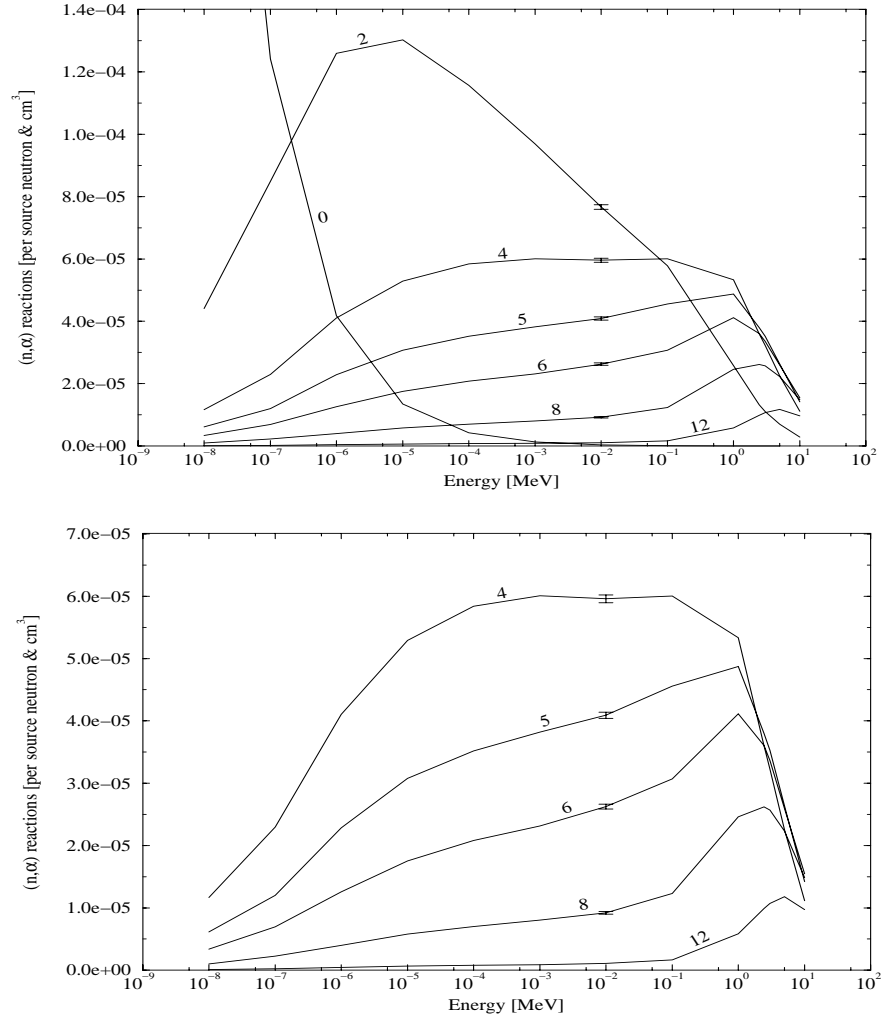Figure 12: *(n,α) reaction rates of graphite moderating BF$_3$ as function of incident neutron energy for different moderator thicknesses given in cm. The average relative error in the calculations is about 5 %. The lower picture shows only a few of the response curves in order to get a better separation of the most interesting ones.*

in Appendix A), a much thicker moderator is needed to slow down the
fast fusion neutrons. As also shown, the thermal neutrons are not lost
through absorption at the same rate for carbon as for polyethylene when
the moderator thickness is increased. This is because graphite also has a
much smaller absorption cross section than polyethylene (see Figure 28
in Appendix A). This results in a more flat response function over a
wider energy range for a thick moderator at higher energies. This is
illustrated in the lower picture of Figure 12. A moderator thickness of
32 cm gives the desired flat response from about 10 keV up to 3 MeV.

The detector response function of a 32 cm thick graphite moderating
BF$_3$-counter is shown together with the elastic scattering cross section
of graphite in Figure 13. The lowest energy point is 10 keV and again it
can be seen that the response function is relatively flat between 10 keV
and 3 MeV except where the resonances occur in the elastic scattering
cross section.

At the resonances, the first scattering occurs very close to the mod-
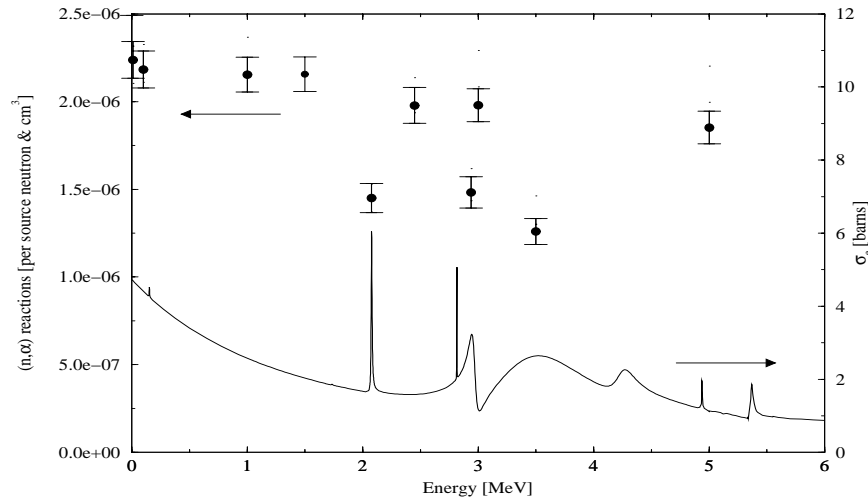
Figure 13: *The dots show the (n,α) reaction rates of a 32 cm thick
graphite moderating BF$_3$-counter as function of incident neutron energy.
The lower curve shows the elastic scattering cross section of graphite as
function of neutron energy.*

erator surface. When the neutrons loose their initial energy in this first scattering, the scattering length is reduced by 40 to 70 per cent. The net result is an increased probability at the resonances for the neutrons to escape the moderator and not to reach the detector. In the thermal energy range however where the elastic scattering cross section is high but continuous, the first scattering also occurs near the moderator surface. However, when the initial energy is lost here, the scattering length is instead constant or increased and thus the probability of the neutron reaching the detector increases.

Because the resonances are very narrow and the main part of the fusion neutrons have an energy of 2.45 MeV the influence of the resonances on the detector response function is negligible when the detector is placed in a real fusion neutron flux. Around 2.45 MeV the elastic scattering cross section of graphite is continuous and most of the neutrons will not be influenced by the resonances.

5.2   Thermal fission chambers

The fission cross section of ^{235}U shows the characteristic $1/v$ dependence at low energies, resonances at intermediate energies, and a smooth curve at high energies where individual resonances overlap [6]. This is shown in Figures 23 and 25 in Appendix A. There are small peaks in the cross section around 0.3 eV and 1 eV. Figure 14 shows detector response functions of polyethylene moderating fission chambers coated with ^{235}U. When there is moderating material the peaks at 0.3 eV and 1 eV, and the resonances level out and a mean cross section is exhibited. This is obvious from the fact that the curves behave almost exactly as in the case of polyethylene moderating BF$_3$-counters, and that ^{10}B also has a smooth $1/v$ dependent (n,α) cross section (see Figure 24 in Appendix A).

The fission cross section of ^{239}Pu, shown in Figures 23 and 26 in Appendix A, has the same behavior as ^{235}U except for a larger peak around 0.3 eV. Figure 15 shows detector response functions of polyethylene moderating fission chambers coated with ^{239}Pu. For the bare core detector a resonance is clearly seen at 100 eV. The response functions behave the same way as for the polyethylene moderating BF$_3$-counters and ^{235}U-fission chambers. This indicates even stronger that the fission cross section exhibited when the moderator is added is a mean cross section.
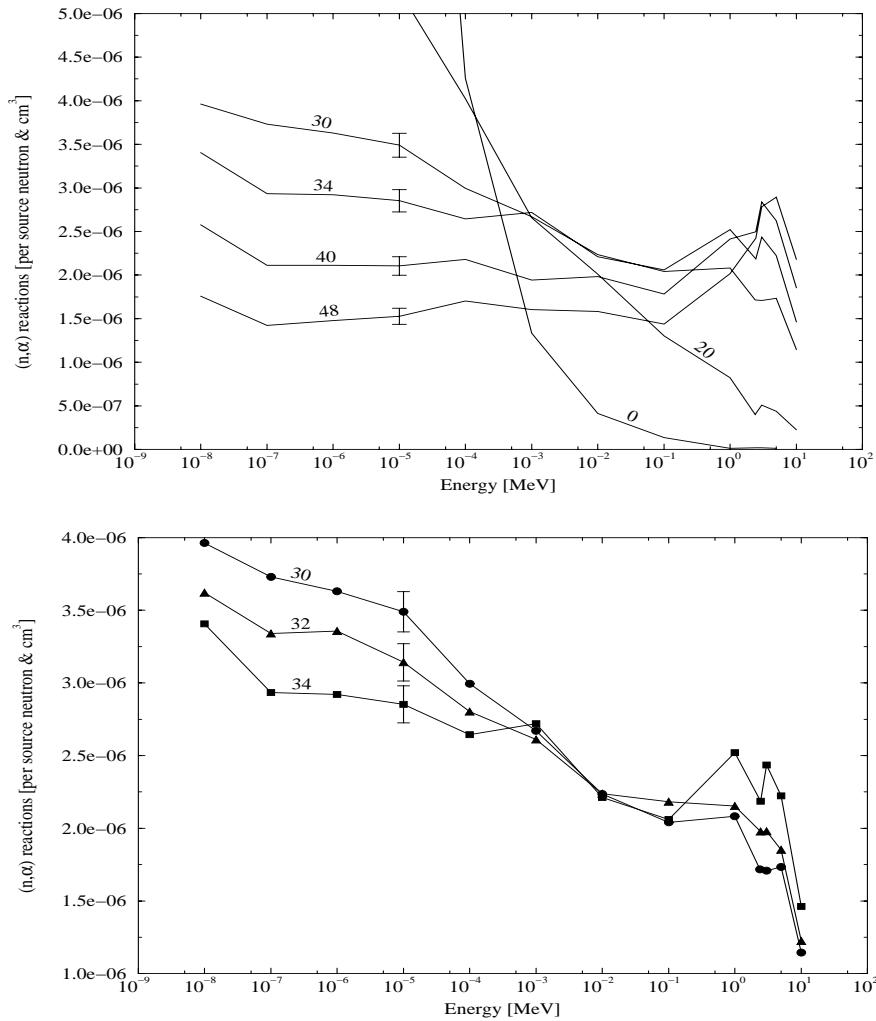
Figure 14: *(n,f) reaction rate of polyethylene moderating ^{235}U as func-
tion of incident neutron energy for different moderator thicknesses given
in cm. The average relative error in the calculations is about 1.5 %. The
lower picture shows only a few of the response curves in order to get a
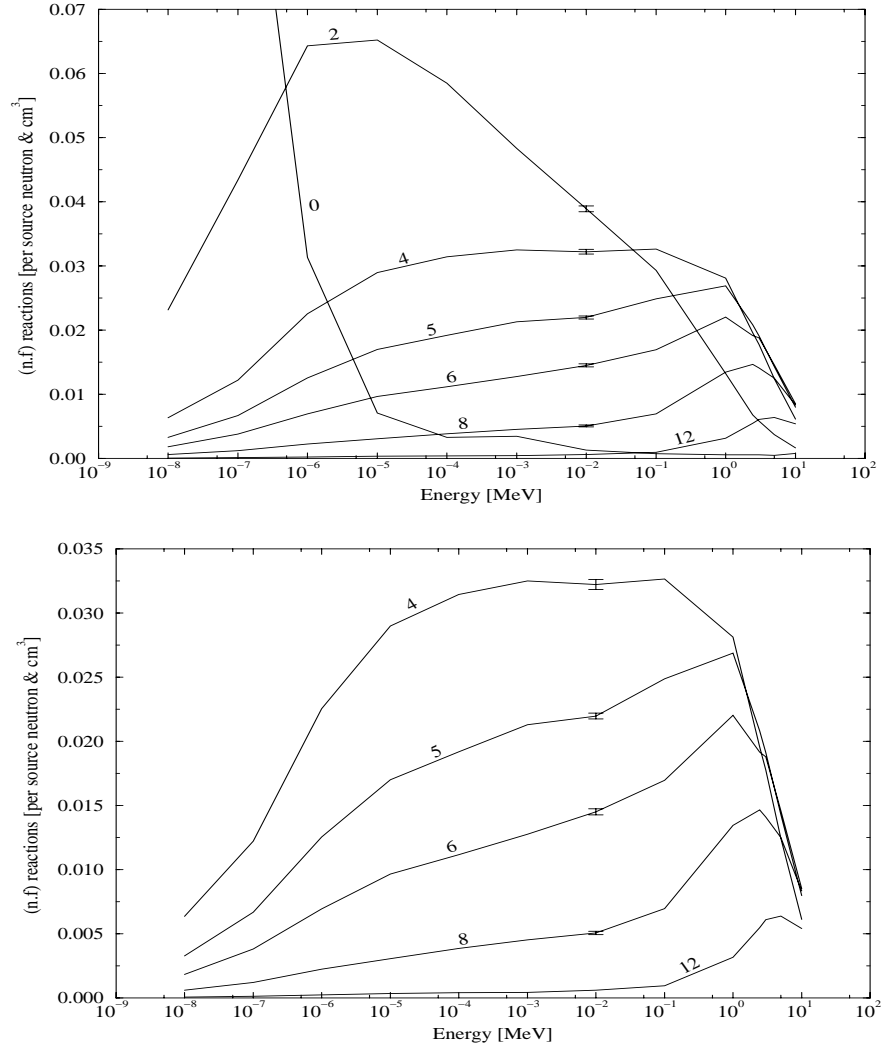better separation in the high energy interval.*
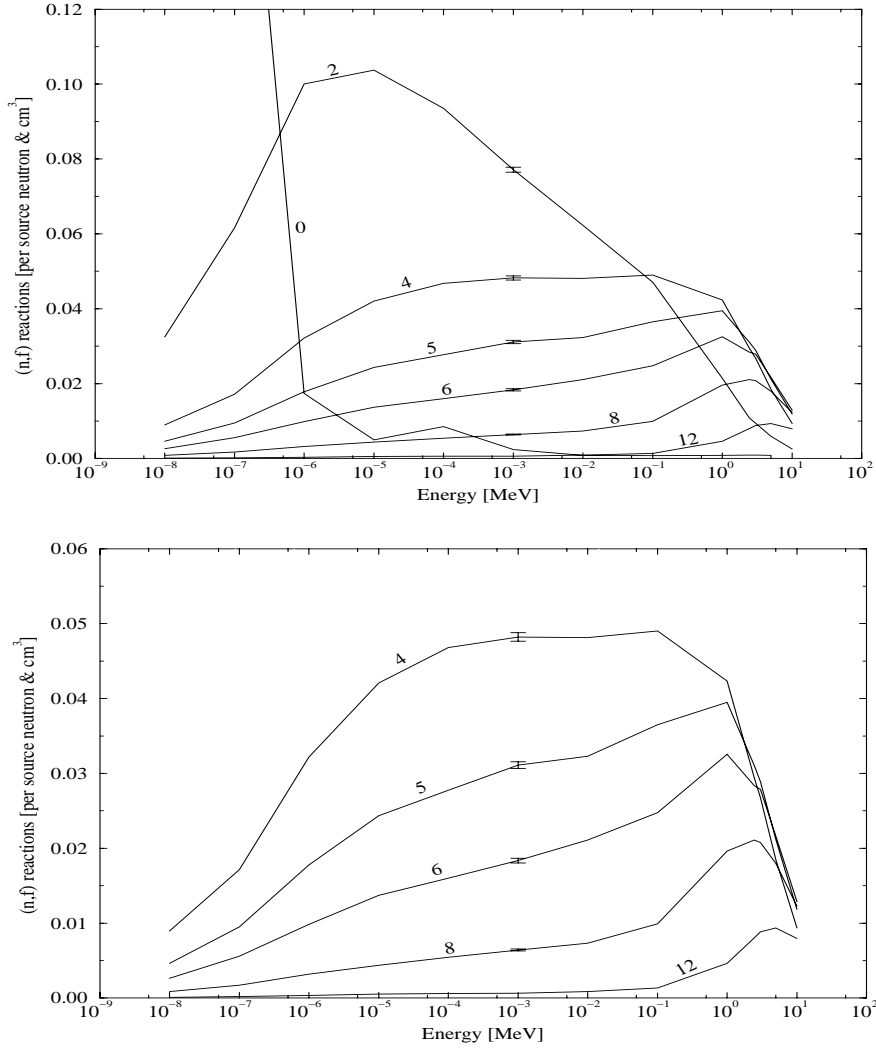
Figure 15: *(n,f) reaction rates of polyethylene moderating ^{239}Pu as function of incident neutron energy for different moderator thicknesses given in cm. The average relative error in the calculations is about 1.5 %. The lower picture shows only a few of the response curves in order to get a better separation in the high energy interval.*

It has been shown that the the fission cross sections of ^{235}U and ^{239}Pu act as mean cross sections when a moderator surrounds the fission chambers. The net result is that the response function of a fission chamber behaves the same way as for a BF$_3$-counter, and therefore response functions of graphite moderating fission chambers are calculated only for the most preferable moderator thickness, i.e. 32 cm. The results are shown in Figure 16. Again the response is sufficiently flat from 3 MeV down to 10 keV.
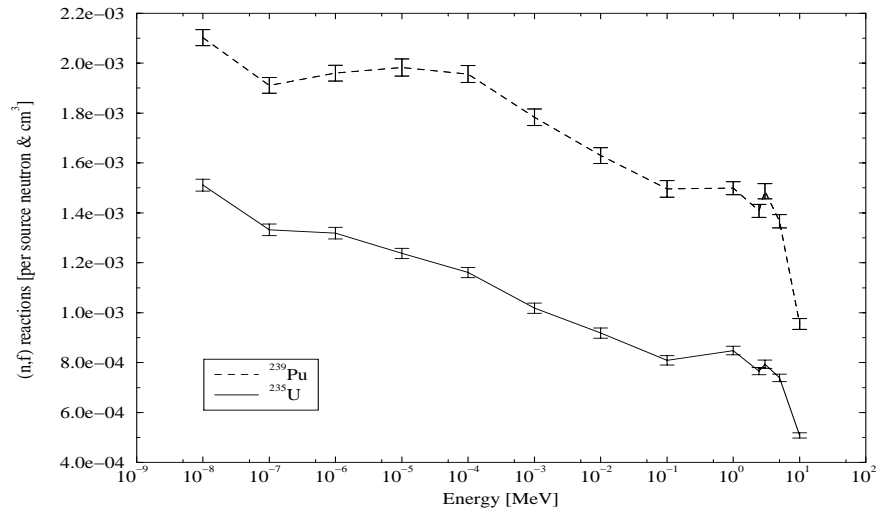
Figure 16: *(n,f) reaction rates of 32 cm thick graphite moderating ^{235}U and ^{239}Pu as function of incident neutron energy.*

5.3   Fast fission chambers

Figure 17 shows the detector response functions of two fast fission chambers coated with ^{238}U and ^{237}Np respectively. Since the detectors do not have any moderator there is a single curve for each detector and the response functions follow the fission cross sections (see Figure 27 in Appendix A) as can be expected. The fast fission detectors have a very flat response function and can be used as threshold detectors, detecting only fast neutrons, which would be excellent for the detection of fusion neutrons.
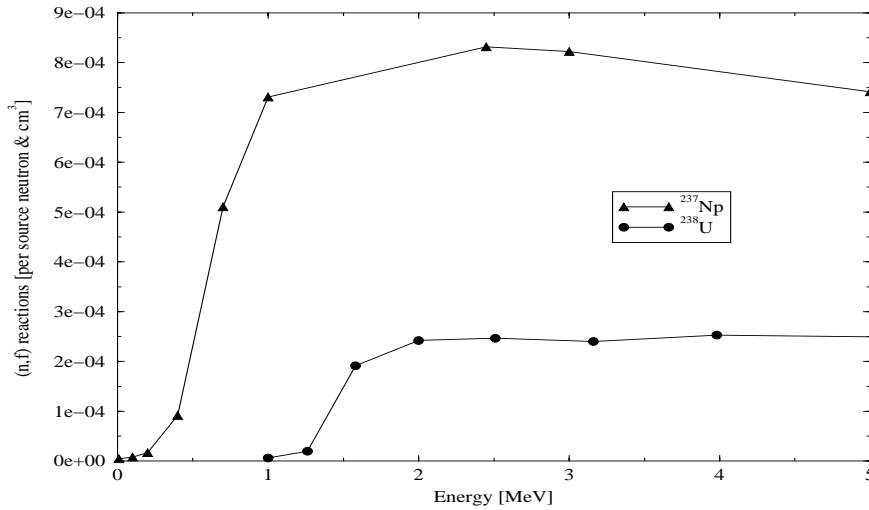
Figure 17: *(n,f) reaction rates of ^{237}Np and ^{238}U respectively as function of incident neutron energy. The relative errors in the calculations are less than the line with in the picture.*

The fast fission chambers require a special type of neutron source[6] to be calibrated for 2.45 MeV fusion neutrons. This is costly and less accurate than a more conventional neutron source, for example californium which has a very well known energy spectra. This and the restrictions on handling fissile materials probably exclude fast fission chambers in the W7-X project. Another fact is that the count rate of a fast fission chamber will be much lower than for a BF_3-counter or a thermal fission chamber. This is partially because the detector is very small since there is no moderator, and partially because the fission cross section is hundred to thousand times smaller than in a thermal neutron detector. It can be seen comparing the cross section in Figures 23 and 27 in Appendix A. As discussed in the beginning of this chapter the neutron field decreases with the distance to the source and thus fewer neutrons will reach a smaller detector.

---

[6] Practical neutron sources do not exist in the same sense that, for example, gamma-ray sources do. The possible choices for neutron sources are much more limited and are based on either spontaneous fission (e.g. Californium) or on nuclear reactions for which the incident particle is either the product of a conventional decay process or an artificially accelerated particle (e.g. fusion). Neutron sources are described in most nuclear physics and radiation detection books, see for instance G. F. Knoll [7].

5.4   Comparison between different detectors and moderators

As already mentioned the cross sections of ^{235}U and ^{239}Pu average out to give a similar $1/v$ dependent cross section as ^{10}B when a moderator is applied. This results in the same type of response functions when using the same moderating material in the thermal fission chambers as in the BF$_3$-counters.

When the reaction rates of the BF$_3$-counter are compared with the fission chamber's reaction rates the fission chambers appear to be the most efficient. This is a matter of how the detectors are compared. The reaction rates are calculated per volume unit (i.e.   cm^3). In order to compare two detectors with the same moderator thickness, the reaction rates should be multiplied with the volume of the detecting material. The volume of the BF$_3$-gas, in the BF$_3$-counter, is 192.4 cm^3 while the volume of the fissile material in the fission chambers is only 0.013 cm^3. This makes the BF$_3$-counters about 25 times as efficient as the thermal fission chambers. This is illustrated in Figure 18 when the BF$_3$-counter is compared with the thermal fission chambers. All three detectors have a 32 cm thick graphite moderator.
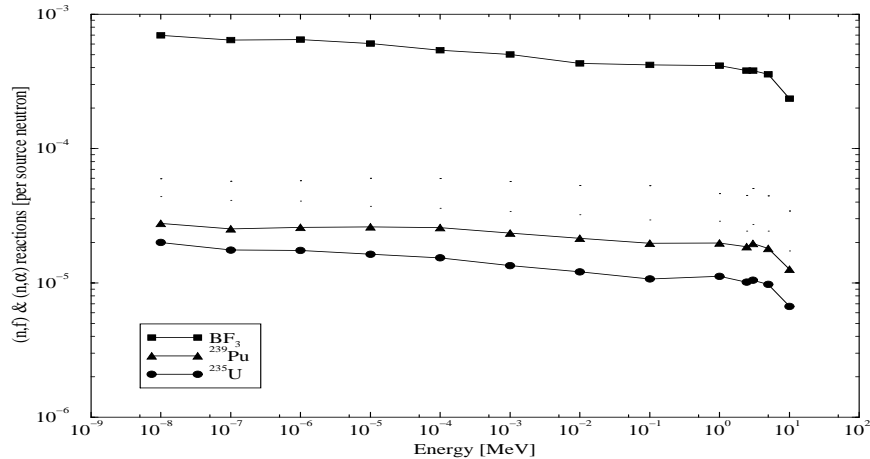
Figure 18: *(n,α) reaction rates of BF$_3$ and (n,f) reaction rates of ^{235}U and ^{239}Pu as function of incident neutron energy. All three detectors have a 32 cm thick graphite moderator. The reaction rates are multiplied with the volume of the detecting material.*

It can be discussed how the different detectors should be compared. By looking at the reaction cross sections in Figure 23 in Appendix A, it is clear that ^{10}B is the most efficient detector material, if the detectors contain the same number of atoms. This is a detector design problem. The BF$_3$-counter contains BF$_3$-gas which is limited in the gas pressure. Also, the boron in the BF$_3$-gas can not be enriched to contain pure ^{10}B. The fission chambers are limited in the thickness of the fissile material. The detectors and their limitations are discussed in Appendix C.

In Figure 19 is the response function of a 4 cm thick polyethylene moderating BF$_3$-counter shown together with the response functions of ^{238}U and ^{237}Np. The figure illustrates that a combination of two detectors, one BF$_3$-counter and one of the fast fission chambers, can be used to obtain the desired flat response over a wide energy range. In order to determine how the two detectors can be combined to give this response, further simulations are needed.
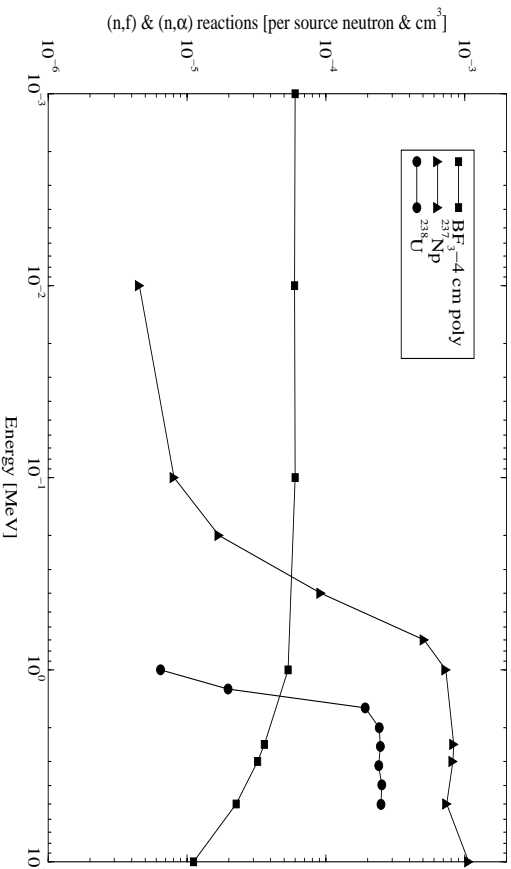
Figure 19: (n,α) reaction rates of 4 cm thick polyethylene moderating BF$_3$ and (n,f) reaction rates of ^{238}U and ^{237}Np as function of incident neutron energy. The fast fission chambers have no moderator.

As already discussed in Section 5.3, it will probably not be possible to have any fast fission chambers in the W7-X project. If a fast fission chamber, however, can be used together with a BF_3-counter or a thermal fission chamber, the size of the detector will have to be increased. As also discussed in Section 5.3, this is because the count rate of the fast fission chambers will be many orders of magnitude smaller than the count rate of the BF_3-counter. Another way to reduce this effect is to reduce the content of ^{10}B in the BF_3-gas, or possibly also to use several detectors.

6 Detector efficiency

In this section absolute efficiencies of the BF_3-counter are calculated for various BF_3-gas pressures. Absolute efficiencies of fission chambers are also discussed. As already shown in Section 5 the thermal fission chambers behave similar to the BF_3-counter when a moderator is applied.

The effect of different neutron spectra and moderators on the detector efficiency of BF_3-counters is also investigated in this section. Results are presented as function of moderator thickness for different neutron energy spectra incident on the moderator. The moderating materials polyethylene, water, graphite, heavy water and beryllium are compared.

6.1 Absolute detector efficiency

Relative detector efficiencies of BF_3-counters at various BF_3-gas pressures as function of neutron energy incident on the detector surface are shown in Figure 20. The maximum efficiency of 100 % is reached when every incoming neutron cause a (n,α) reaction in ^{10}B. Other forms of neutron capture are not considered when the efficiency is calculated.

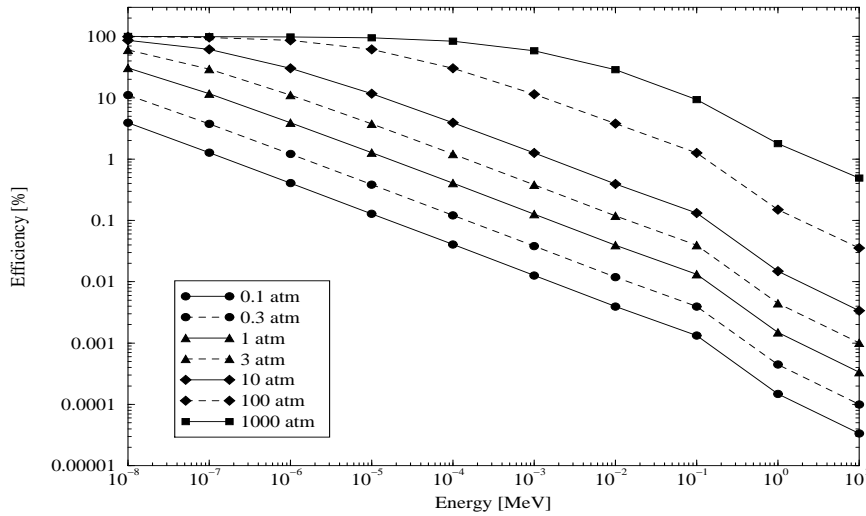Figure 20: *Detector efficiency of BF_3, for different BF_3-gas pressures, as function of incident neutron energy. Mono-energetic neutrons are incident on the detector surface.*

Their contributions however, are very small for ^{10}B. It can be seen that the curves flatten out as maximum efficiency is reached, i.e. the system gets self moderated. For a gas pressure of 1 atm, which is the BF_3-counter considered throughout this thesis, the detector efficiency is about 30 % for thermal neutrons. The pressure can be raised somewhat to receive a more efficient detector. There are however limitations to the pressure in a BF_3-counter, a matter which is discussed in Appendix C.1. A pressure of 1000 atm is outrageous since the BF_3 would be in solid state.

Calculating the efficiency of a fission chamber is more complicated than in the case of a BF_3-counter. It is not only dependent on the number of fissile atoms available. In a fission chamber, the thickness of the coating fissile isotope must be limited so that the fission products can be detected properly, as described in Appendix C.2. The neutron absorption cross section of a fissile isotope consists of two parts, capture and fission. In a fissile material a substantial amount of the neutrons are captured and thus do not cause fission reactions. This fraction is energy dependent and varies from one isotope to another. If no capture is considered and nor the thickness of the coating, the thermal fission chambers (used in this work) have an efficiency of just over 1 %. The fast fission chambers have an efficiency less than 0.002 %. All the detectors have a 0.6 μm thick coating of the fissile isotope.

6.2   Effect of different neutron spectra and moderators

Figure 21 shows the detector count rate for direct fusion neutrons incident on the moderator surface as function of the moderator thickness. Moderators used are polyethylene, water, heavy water, beryllium and graphite.

Water and polyethylene behave similarly. The neutrons loose their energy mainly by scattering against hydrogen and not very much moderating material is needed in order to slow down the fast fusion neutrons, and to reach the maximum efficiency. On the other hand for increased moderator thickness the efficiency drops quickly again. This is due to the relative high absorption cross section of water and polyethylene in the thermal energy region. Heavy water, beryllium and graphite behave similarly although the graphite has to be at least 30 cm thick to slow down the fusion neutrons efficiently. Graphite has a very low neu-
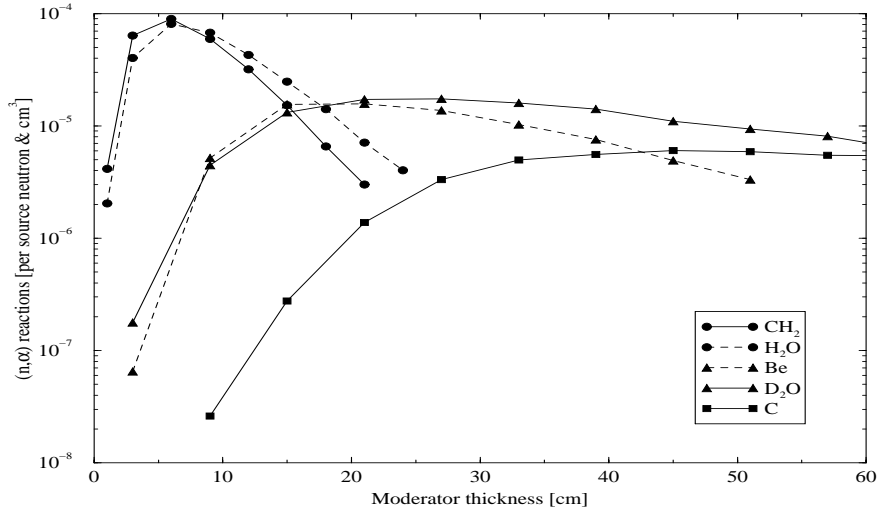
Figure 21: *(n,α) reaction rates of BF₃ as function of the moderator thickness for direct fusion neutrons. The moderating materials are water, polyethylene, heavy water, beryllium and graphite. The neutrons are incident on the moderator surface and have the energy distribution of D-D fusion with a plasma temperature of 3 keV.*

tron absorption cross section, resulting in an almost flat curve once the neutrons have become thermal. This suggests that the count rate of a graphite moderating detector is very tolerant to changes in the incident neutron spectrum and thus will be a suitable moderator for obtaining a flat detector response, as already shown in Section 5.

In all other calculations performed in this work, polyethylene and graphite have been chosen because they, as just shown above, behave quite differently as moderating materials. They have also been selected for practical reasons. Water and heavy water are not very convenient in detector configurations since they are liquids and beryllium is a very poisonous substance.

Detector count rates as function of the thickness of the moderators polyethylene and graphite are shown in Figure 22. The detector is here placed in the neutron field of different torus configurations. When the floor is added to the Simple torus model, neutrons are scattered from
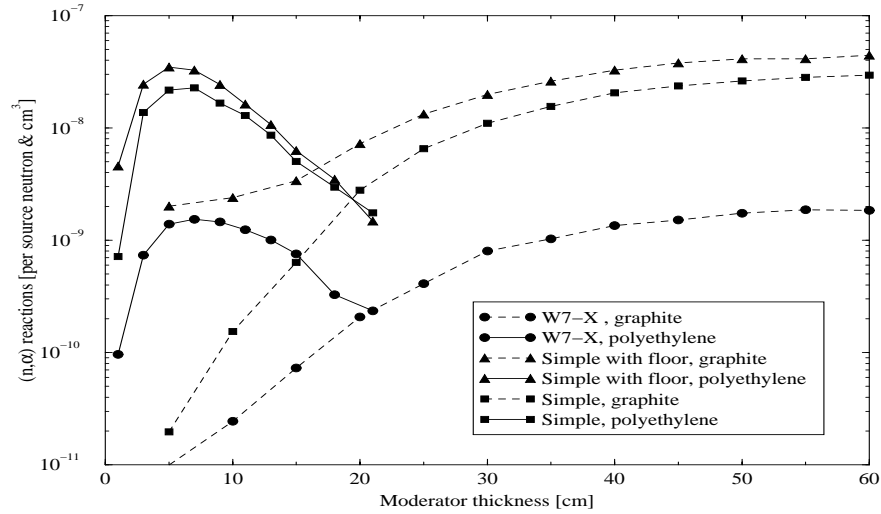
Figure 22: *(n,α) reaction rates of polyethylene and graphite moderating*
BF$_3$-counters as function of the moderator thickness for different tori
configurations.

the floor and the neutron flux around the detector is increased by about
70 %. Scattered neutrons have lost a lot of their initial energy and thus
have larger probability to cause (n,α) reactions in the detector for a thin
moderator. This is particularly obvious for a graphite moderator, where
the count rate for a 5 cm thick moderator is hundred times higher when
the floor is added to the model.

In the W7-X model the neutron flux around the detector is only about
5 % of the flux generated by the Simple model without the floor. The
W7-X model is composed of a lot more material than the Simple model,
resulting in large absorption in the torus walls and that neutrons can
escape the torus almost only through the ports. This also results in a
neutron flux increase of less than 10 % when a floor is added to the
W7-X model.

It can be seen from Figures 21 and 22 that the count rate of the graphite
moderating detector is raised significantly when the detector is placed
in an inhomogeneous neutron field from a stellarator. The reasons for

this is that the neutrons have a larger probability to reach the detector, as described in detail in the beginning of Section 5.

As also indicated in Figure 22 the count rate of a graphite moderating detector tends to increase more and more as the moderator thickness increases. It is not important to determine the most efficient moderator thickness since the previous response calculations have shown that a slightly under moderated system (i.e. 32 cm of graphite) gives the desired flat response function.

7   Final calculations

In the final calculations the absolute response function is calculated for a BF_3-counter with a 32 cm thick graphite moderator. Detector count rates are calculated and compared in three different surrounding environments. First, only the W7-X torus. Second, the torus and the floor. Third, the torus and the floor, walls and ceiling (i.e. reactor hall).

The graphite moderated BF_3-counter is selected because it is the most suitable detector and moderator combination. BF_3 is the most efficient detector material and a 32 cm thick graphite moderator gives a sufficient flat response according to results obtained in Sections 5 and 6.

The W7-X torus model is chosen since it best describes the planned W7-X stellarator experiment as discussed in Section 4.

The results are presented in Table 2.

Environment	(n,α) reactions per source neutron	Statistical error
torus	$1.59592 \cdot 10^{-7}$	1.85 %
torus & floor	$1.68323 \cdot 10^{-7}$	1.81 %
torus & reactor hall	$1.70902 \cdot 10^{-7}$	1.79 %

Table 2: *Total number of (n,α) reactions in a 32 cm graphite moderating BF_3-counter for different environmental configurations.*

It can be seen that the influence of the reactor hall on the detector count rate compared to just the floor is so small that it is within the statistical error and thus can not be determined. This was obtained already in Section 4.2. However, in Section 4.1 it was also shown for the Simple torus model that as much as 42 % of the neutrons reaching the detector had been scattered in the floor. In case of the W7-X torus the detector count rate will only be increased with about 5-7 % due to neutron scatter in the concrete floor, walls and ceiling.

If W7-X will generate 10^{12} to 10^{16} neutrons per second the absolute detector count rate will be $2 \cdot 10^5$ to $2 \cdot 10^9$ neutrons per second.

8 Conclusions

The Monte-Carlo method is an effective tool to simulate the neutron production and transport in the W7-X stellarator and to select a suitable detector and moderator combination.

Neutron spectra calculations and comparison of different torus models quantifies the impact of the modeling of the stellarator and surrounding floor, walls and ceiling (i.e. reactor hall) on the neutron spectra.

In the Simple torus model consisting only of a 10 cm thick stainless steel vacuum vessel the main part of the neutrons are scattered straight through the vessel. The spectrum is calculated with and without ports. Excluding ports results in a 17 % decrease of the 2.45 MeV fusion neutrons. It is also shown that 42 % of all neutrons reaching the detector have been scattered in the floor.

The W7-X model has a 70 cm thick vacuum vessel and thus the majority of the neutrons generated in the stellarator are captured and scattered within the vessel, and most of the detected neutrons escape through the ports. This also demonstrates that the location of the ports is important for the count rate. The count rate will increase by about 5-7 % due to neutrons scattered in the floor.

Response function simulations show that a cylindrical shaped BF_3-counter or thermal fission chamber with a 32 cm thick graphite moderator gives the desired flat response function. For polyethylene moderating detectors it is possible to maintain a flat response only up to about 1 MeV which is not satisfactory. Use of fast fission chambers will only give a flat response above 1-2 MeV and will thus not account for the major part of scattered neutrons.

Calculation of the absolute detector efficiency of BF_3-counters shows that polyethylene and graphite gives about the same count rate for the optimum moderator thickness when placed in an inhomogeneous neutron field from a stellarator.

Finally, the absolute response function was calculated for a BF_3-counter with a 32 cm thick graphite moderator and compared for three different surrounding environments. First, only the W7-X torus. Second, the

torus and the floor. Third, the torus and the floor, walls and ceiling. The results show that a stellarator generating 10^{12} to 10^{16} neutrons per second will give an absolute detector count rate of $2\cdot10^5$ to $2\cdot10^9$ neutrons per second. Scattering of neutrons in the concrete floor will increase the detector count rate by about 5-7 %. The impact of walls and the ceiling is negligible.

The very large count rate of $2\cdot10^5$ to $2\cdot10^9$ neutrons per second is way beyond the capability of any commercial detector and thus can fission chambers with low efficiency very well be used giving a satisfactory count rate. This concludes that a 32 cm graphite moderating BF_3-counter as well as any thermal fission chamber can be used to achieve sufficient flat response and highest possible count rate. Due to the significant count rate and the fact that the largest fraction of neutrons leaving the stellarator are fast fusion neutrons, a fast fission chamber will probably be efficient enough. The advantage of a fast fission chamber is that it gives a very flat response, however only above 1-2 MeV.

In order to achieve a flat response function from thermal energies up to the fast region a polyethylene moderating BF_3-counter or thermal fission chamber can be combined with a fast fission chamber. This however requires further investigation and simulations which are beyond the scoop of this work.

9 Acknowledgment

A   Cross sections

In this section are the reaction cross sections of the detector materials plotted. Some important cross sections of the moderators are also shown. The Figures are plotted by MCNP version 4b with data taken from ENDF/B-VI.

Figure 23:   Show the fission cross sections of ^{235}U and ^{239}Pu, and the (n,α) reaction cross section of ^{10}B as function of energy in the energy range from 0.01 eV to 10 eV.

Figure 24:   Shows the (n,α) reaction cross section of ^{10}B as function of energy.

Figure 25:   Shows the fission cross section of ^{235}U as function of energy.

Figure 26:   Shows the fission cross section of ^{239}Pu as function of energy.

Figure 27:   Show the fission cross sections of ^{237}Np and ^{238}U as function of energy in a linear energy scale.

Figure 28:   Show the absorption cross sections of graphite and polyethylene as function of energy.

Figure 29:   Show the elastic scattering cross sections of graphite and polyethylene as function of energy. This is shown in a logarithmic scale as well as in a linear scale to resolve the resonances.
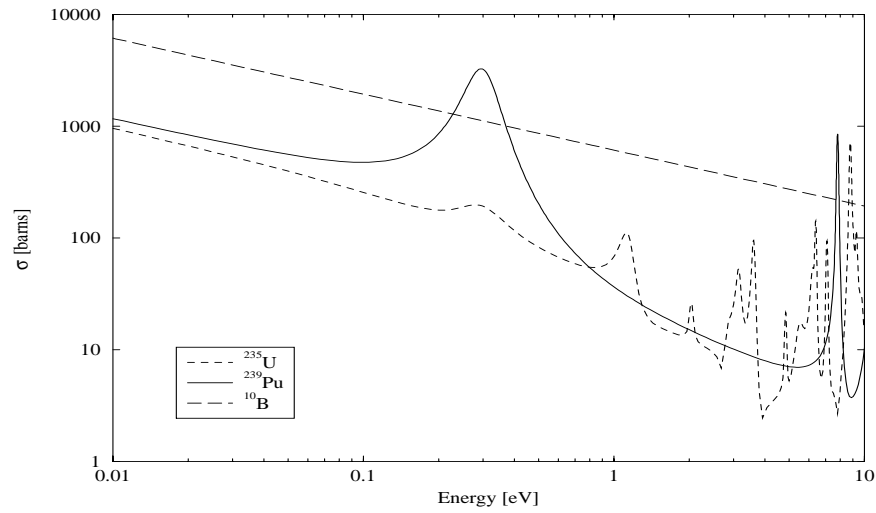
Figure 23: *Fission cross sections of ^{235}U and ^{239}Pu, and (n,α) reaction cross section of ^{10}B as function of energy in the low energy range, plotted by MCNP version 4B with data taken from ENDF/B-VI.*
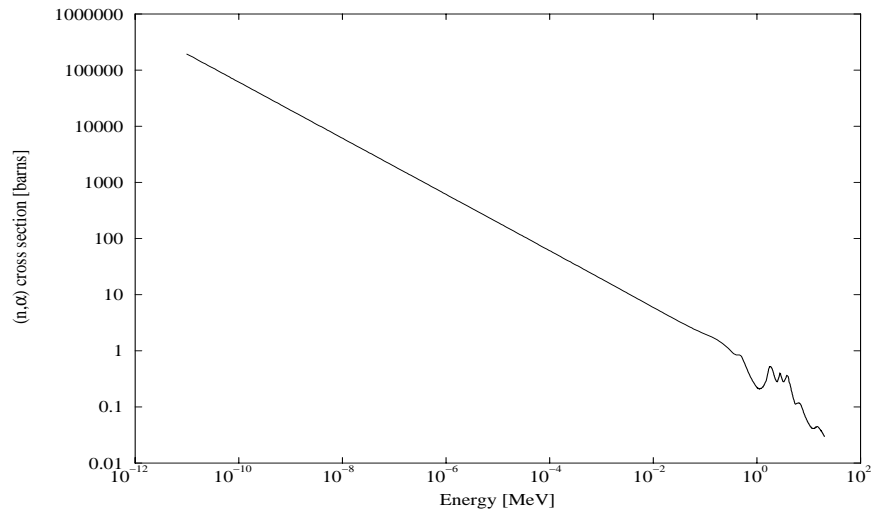
Figure 24: *(n,α) reaction cross section of ^{10}B as function of energy, plotted by MCNP version 4B with data taken from ENDF/B-VI.*
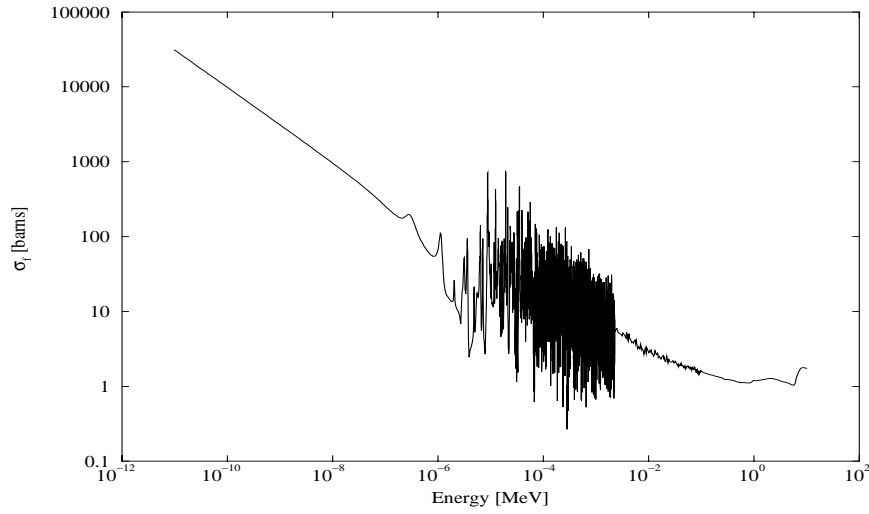
Figure 25: *Fission cross section of ^{235}U as function of energy, plotted by MCNP version 4B with data taken from ENDF/B-VI.*
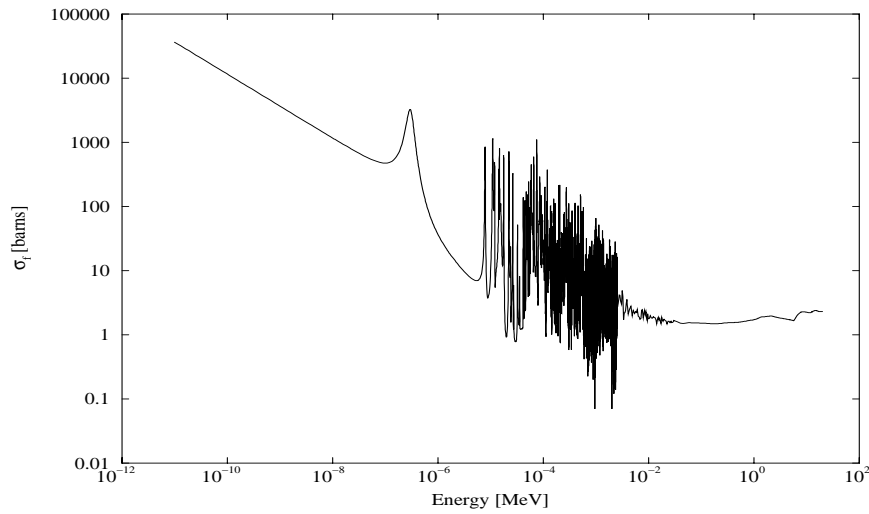
Figure 26: *Fission cross section of ^{239}Pu as function of energy, plotted by MCNP version 4B with data taken from ENDF/B-VI.*
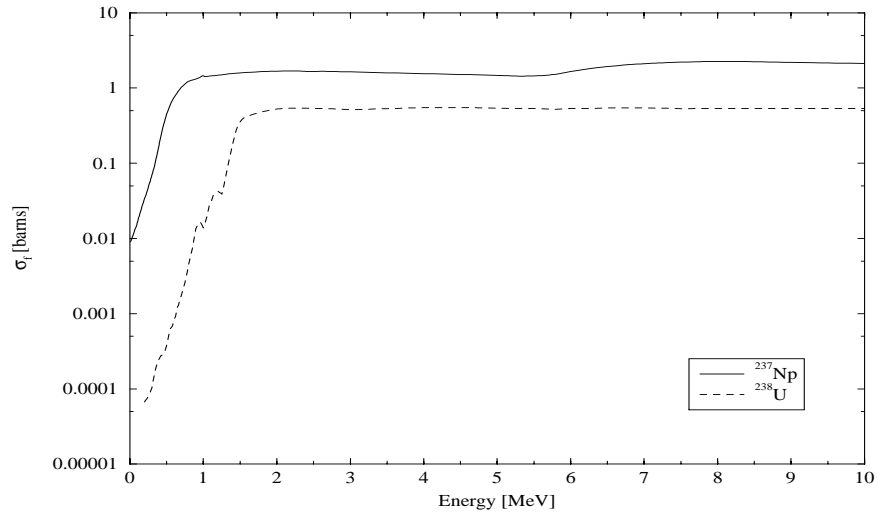
Figure 27: *Fission cross sections of ^{237}Np and ^{238}U as function of energy, plotted by MCNP version 4B with data taken from ENDF/B-VI.*
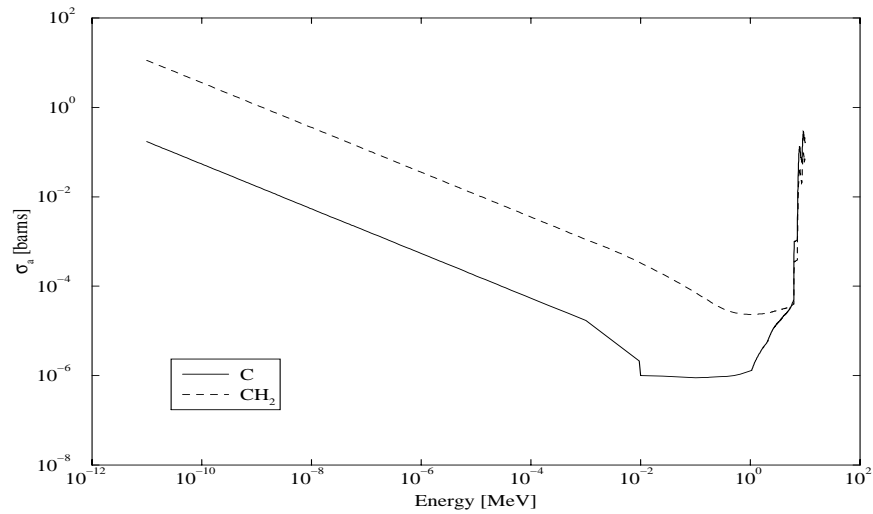
Figure 28: *Absorption cross sections of graphite and polyethylene as function of energy, plotted by MCNP version 4B with data taken from ENDF/B-VI.*
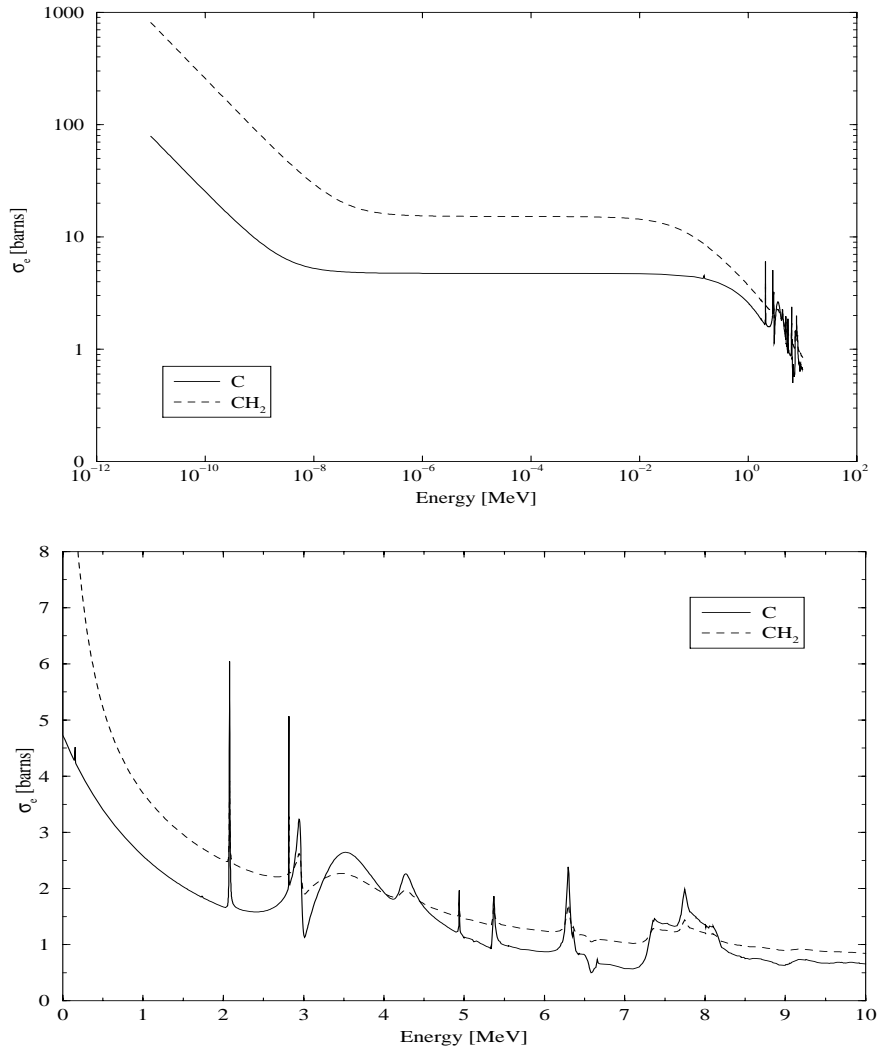
Figure 29: *Elastic scattering cross sections of graphite and polyethylene as function of energy, plotted by MCNP version 4B with data taken from ENDF/B-VI. Top: plotted in a logarithmic scale. Bottom: plotted in a linear scale to resolve the resonances.*

B Tables of materials

The material compositions, cross sections and other essential data of the materials used in the calculations are presented in Tables 3-10 below.

CONCRETE (KENO) [8]		
(Regular Concrete Standard Mix)		
Density = 2.3 g/cm^3		
Nuclide	**Wt. Frac.**	**Cross sect.**
H	0.010	1001.60c
O	0.532	8016.60c
Si	0.337	14000.60c
Al	0.034	13027.60c
Na	0.029	11023.60c
Ca	0.044	20000.60c
Fe	0.014	26000.55c

Table 3: *Material composition and cross sections of the concrete used in floor, walls and ceiling.*

STAINLESS STEEL 304 [8]		
Density = 7.92 g/cm^3		
Nuclide	**Wt. Frac.**	**Cross sect.**
Fe	0.695	26000.55c
Cr	0.190	24000.50c
Ni	0.095	28000.50c
Mn	0.020	25055.50c

Table 4: *Material composition and cross sections of the stainless steel vacuum vessel of the Simple torus model.*

| STAINLESS STEEL | | |
| Density = 20.6 g/cm^3 | | |
Nuclide	Wt. Frac.	Cross sect.
Fe	0.040	26054.60c
Fe	0.690	26056.60c
Fe	0.020	26057.60c
Cr	0.010	24050.60c
Cr	0.150	24052.60c
Cr	0.015	24053.60c
Ni	0.050	28058.60c
Ni	0.020	28060.60c
Ni	0.005	28062.60c

Table 5: *Material composition and cross sections of the stainless steel vacuum vessel of the W7-X torus model.*

| STAINLESS STEEL | | |
| Density = 22.4 g/cm^3 | | |
Nuclide	Wt. Frac.	Cross sect.
Fe	0.040	26054.60c
Fe	0.660	26056.60c
Fe	0.020	26057.60c
Cr	0.010	24050.60c
Cr	0.160	24052.60c
Cr	0.015	24053.60c
Ni	0.060	28058.60c
Ni	0.025	28060.60c
Ni	0.010	28062.60c

Table 6: *Material composition and cross sections of the stainless steel outer vessel of the W7-X torus model.*

COPPER etc.		
Density = 6.17 g/cm^3		
Nuclide	**Wt. Frac.**	**Cross sect.**
Cu	0.210	26063.60c
Cu	0.090	29065.60c
H	0.0005	1001.60c
C	0.006	6000.60c
Si	0.012	14000.60c
O	0.012	8016.60c
Ni	0.001	26054.60c
Ni	0.140	26056.60c
Ni	0.004	26057.60c
Ni	0.030	28058.60c
Ni	0.020	28060.60c
Mn	0.0044	25055.60c
C	0.00616	6000.60c
Si	0.00572	14000.60c

Table 7: *Material composition and cross sections of the homogeneous mixture of coils, support structure and cladding materials of the W7-X torus model.*

MODERATING MATERIALS			
Material		**Density** $[g/cm^3]$	**Cross sect.**
Water	H_2O	1.00	1001.60c
			8016.60c
Heavy water	D_2O	1.10	1002.60c
			8016.60c
Graphite	C	1.60	6000.60c
Beryllium	Be	1.85	4009.60c
Polyethylene	CH_2	0.92	6000.60c
			1001.60c

Table 8: *Essential data of the different moderating materials.*

BF$_3$ - GAS		
Density = 0.002735 g/cm^3 (1 atm.)		
Nuclide	**Atomic density** $[atoms/cm\ barn]$	**Cross sect.**
^{10}B	$2.429 \cdot 10^{-5}$	5010.60c
F	——	9019.60c

Table 9: *Essential data of the BF$_3$-gas used in the BF$_3$-counters.*

FISSILE MATERIALS			
Nuclide	**Density** $[g/cm^3]$	**Cross sect.**	**Conc.** $[mg/cm^2]$
^{235}U	18.70	92235.60c	1.12
^{238}U	18.90	92238.60c	1.13
^{239}Pu	19.60	94239.60c	1.18
^{235}Np	20.45	93237.60c	1.23

Table 10: *Essential data of the fissile materials used in the different fission chambers.*

C Neutron detection

Since neutrons are uncharged particles they have to be detected through nuclear reactions in which charged particles or photons are produced and in turn recorded by an appropriate detector. Most cross sections for neutron interaction are largest for thermal neutrons and thus thermal neutrons are most efficiently detected. To detect fast neutrons a moderator may be used around the detector to slow down the neutrons.

The discussion about neutron detection in this section is limited to the methods used in this work. For further reading, see several books on radiation detection, for example [7] and [9].
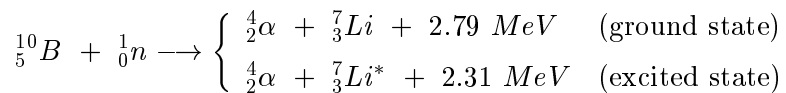
C.1 BF$_3$-counters

The ^{10}B(n,α) reaction is probably the most useful reaction for the conversion of thermal neutrons into directly detectable particles, for three main reasons [9]:

- The (n,α) reaction cross section is large, 3840 barns for thermal neutrons (0.025 eV).

- The cross section is inversely proportional to the neutron speed, i.e.
$$\sigma(n,\alpha) \ \sim \ \frac{1}{v} \ \sim \ \frac{1}{\sqrt{E}}$$

- ^{10}B is a constituent of the compound BF$_3$, which can be used in a proportional gas counter.

The BF$_3$-counter is a *proportional counter*[7] filled with BF$_3$-gas, highly enriched in its ^{10}B concentration. The natural isotopic abundance of ^{10}B is 19.8 %. BF$_3$ serves both as the target for slow neutron conversion into secondary particles as well as a proportional gas. The BF$_3$-counter detects the lithium and alpha particles produced by the reaction

$$^{10}_{5}B \ + \ ^{1}_{0}n \longrightarrow \begin{cases} ^{4}_{2}\alpha \ + \ ^{7}_{3}Li \ + \ 2.79 \ MeV & \text{(ground state)} \\ ^{4}_{2}\alpha \ + \ ^{7}_{3}Li^* \ + \ 2.31 \ MeV & \text{(excited state)} \end{cases}$$

---

[7]To use a gas-filled detector to observe individual pulses, the charge represented by the original ion pairs created within the gas has to be considerably amplified. This is done by the phenomenon of gas multiplication. An excess voltage is applied such that charge multiplication takes place. The number of secondary events created are proportional to the number of initial events, and the detector is therefore known as a *proportional counter*.

When thermal neutrons are used to induce the reaction, about 96 % [7] of all reactions lead to an excited state of ^{7}Li. The excited lithium nucleus quickly returns (i.e. half-life of $\sim 10^{-13}$ s) to the ground state by emitting a gamma ray with energy equal to 2.79 - 2.31 = 0.48 MeV. Because the incoming energy of the slow neutron is much smaller than the reaction Q-value (i.e. 2.31 or 2.79 MeV [7]), it is impossible to extract any information about it by measuring the energies of the reaction products. Thus, the BF$_3$-counter may only be used as a counter and not as a spectrometer.

If the neutron flux is uniform over the detector volume, the relationship between count rate and neutron flux is given by [9]

$$R \text{ (reactions/s)} = V N \int_0^{E_m} \sigma(E)\,\phi(E)\,dE \qquad (1)$$

where

$$
\begin{aligned}
n(E)\,dE &= \text{number of neutrons/m}^3 \text{ with kinetic energy be-} \\
&\quad \text{tween } E \text{ and } E + dE \\
\phi(E)\,dE &= v(E)\,n(E)\,dE = \text{neutron flux of neutrons with} \\
&\quad \text{kinetic energy between } E \text{ and } E + dE \\
v(E) &= \text{neutron speed for energy } E \text{ (m/s)} \\
E_m &= \text{upper limit of neutron energy considered} \\
N &= \text{number of } ^{10}\text{B atoms per unit volume} \\
V &= \text{volume of the counter} \\
\sigma(E) &= \sigma(v) = \text{cross section of the } (n,\alpha) \text{ reaction for} \\
&\quad \text{neutron energy } E
\end{aligned}
$$

The sensitivity of a detector is defined as the ratio [9]

$$S \text{ (counts/s per neutrons/m}^2 = \frac{\text{true net count rate}}{\text{neutron flux}} = \frac{\epsilon_p\,R}{\phi} \qquad (2)$$

where

$$
\begin{aligned}
\epsilon_p &= \text{efficiency of the counter for detection of the charged par-} \\
&\quad \text{ticles produced} \\
R &= \text{reaction rate given by Equation 1} \\
\phi &= \text{neutron flux}
\end{aligned}
$$

The BF$_3$-counter is commercially specified by sensitivity, dimensions, composition and pressure of the filling gas, operating voltage and maximum operating temperature. Some typical specifications are [9]

Sensitivity:	< 1 to 0.005 counts/s per neutrons/m$^2 \cdot$ s.
Dimensions:	Almost any dimensions.
Pressure of BF$_3$:	About 1 to 2 atm. At higher pressures the performance of BF$_3$ as a proportional gas is poor. An increase in pressure requires an increase in the operating voltage.
Operating voltage:	1000 to 3000 V.
Temperature:	Up to about 100°C.

C.2   Fission chambers

Fission chambers can be used for the detection of either fast or thermal neutrons. The isotopes ^{233}U, ^{235}U and ^{239}Pu have large fission cross sections for thermal neutrons and the cross sections are of the $1/v$ type in the low energy range. If ^{238}U, ^{237}Np or ^{232}Th are used as detector material, only fast neutrons with energies above 1 MeV may be detected because the fission cross sections of these isotopes have thresholds around that energy. The fission cross sections are about 500 times smaller than for the isotopes detecting thermal neutrons.

The fission chambers are *ionization chambers*[8] which detect the fragments produced by fission. The fission fragments are massive charged particles (Z $\simeq$ +20e) with kinetic energy 60-100 MeV. The exact identity of the fission products varies from one fission event to another. A typical reaction is [6]

$$^{235}_{92}U \ + \ ^{1}_{0}n \ \longrightarrow \ ^{236}_{92}U^* \ \longrightarrow \ ^{147}_{57}La \ + \ ^{87}_{35}Br \ + \ 2\,^{1}_{0}n$$
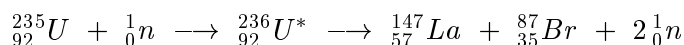
The masses of the two fission fragments, La and Br, are not equal. Unsymmetrical fission such as this is much more likely than fission with two products of equal mass. The mass numbers of the fission fragments lie between 70 and 160. The reactions have very large Q-values (approximately 200 MeV) and like the BF$_3$-counter the fission chambers may only be used as counters and not for detection of the incident neutron

---

[8]The amplitude of the signal is proportional to the number of ions formed, and thus to the energy deposited in the detector. No charge multiplication takes place and therefore the signal is not very large and only strongly ionizing particles such as alphas, protons and heavy ions may be detected.

energy. Also as a result of the large Q-values, the detector output signal can quite easily be discriminated from signals generated by alpha, beta and gamma rays, which are always present[9].

In most commercial fission chambers, the interior surface of the counter is coated with a fissile isotope as shown in Figure 30. The count rate of a fission chamber is proportional to the fission rate, which in turn is proportional to the neutron flux. The relationship between these quantities is similar to the equations given for the BF_3-counter in Section C.1 [9]. The thickness of the coating should be less than the range of the fission fragments so that every fission can be detected. It must also be limited such that the pulse will be large enough to discriminate the alpha, beta and gamma rays.
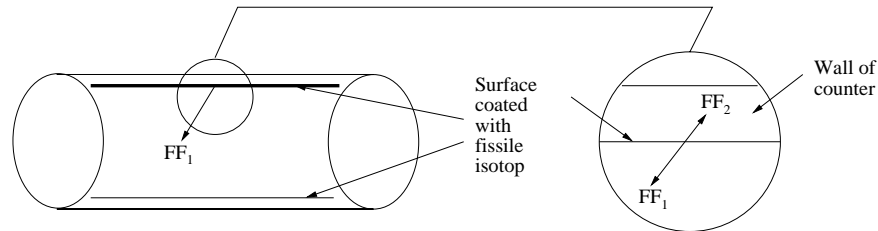
Figure 30: *A fission chamber. The interior surface of the detector is coated with a fissile isotope. When fission takes place, the fission fragments, FF_1 and FF_2, are emitted in opposite directions. One stops in the wall and the other is ionized and detected [9].*

---

[9]Almost all fissile nuclides are naturally alpha radioactive. Beta and gamma rays can be emitted promptly in the fission reaction or delayed by the fission fragments.

D   Controlled Fusion

Nuclear fusion is a process where two light nuclei are combined into a heavier one while energy is released. This is a naturally occurring process which takes place continuously in the sun and stars.

Many different nuclear fusion reactions occur in the sun and other stars. To produce net power on earth only a few such reactions are of practical interest. These all involve the hydrogen isotopes deuterium (^{2}H or D) and tritium (^{3}H or T) and are given by [10]:

$$
\begin{array}{lllllllll}
^2H & + & ^2H & \longrightarrow & ^3He & + & n & + & 3.3 & MeV & \text{(D-D reaction)} \\
^2H & + & ^2H & \longrightarrow & ^3H & + & p & + & 4.0 & MeV & \text{(D-D reaction)} \\
^2H & + & ^3H & \longrightarrow & ^4He & + & n & + & 17.6 & MeV & \text{(D-T reaction)}
\end{array}
$$
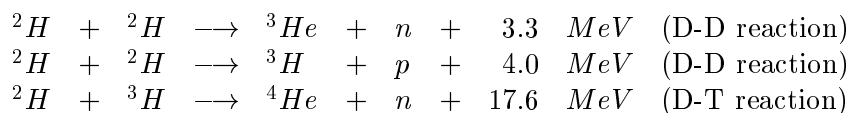
The most suitable one is the D-T reaction which can occur at the lowest temperatures.

For energy production, fusion reactions must take place at very high temperatures (i.e. temperatures of the order of 10^8 K and mean particle kinetic energies of 10 keV). The particles must be in sufficient number (high density) and well confined for a long enough time. At these simultaneous conditions the electrons are stripped from their nuclei, and the fuel consists of a mixture of clouds of positive ions and negative electrons but is overall electrically neutral. This represents a fourth state of matter called a plasma.

Since nuclei carry positive charges, they repel one another. In order to fuse two nuclei they have to overcome the force of repulsion of the positive charges , the Coloumb barrier. The higher the temperature is the higher the average ion velocity becomes. The fastest ions in the distribution function can thus penetrate the Coloumb barrier. The conditions of plasma density and confinement time express the requirements for a sufficient number of particles to react and to compensate for the external energy used for heating and maintaining the plasma.

D.1   Stellarators and tokamaks

In stellarator fusion experiments the plasma is confined by magnetic fields generated by magnetic field coils outside the plasma region. In a tokamak part of the field is generated by a strong electric current

flowing in the plasma. An advantage of stellarators is that they are operated in steady-state, while tokamaks only work in pulsed mode. Stellarators may thus be the more favorable solution for a future fusion power plant. On the other hand tokamak experiments are one generation ahead of stellarator experiments addressing questions related to plasma physics and fusion technology. For more details concerning the future, advantages and disadvantages of the two concepts see [2].

D.2   Wendelstein 7-X project

W7-X belongs to the new generation of "Advanced Stellarators" [5] where a physically improved magnetic field is generated by 3D shaped coils. The coil system will be composed of 50 non-planar, super-conducting magnetic field coils, see Figure 31. Their purpose is to confine a plasma having temperatures of 20 to 50 million degrees and densities of $2 \cdot 10^{20}$ particles per cubic meter [1].
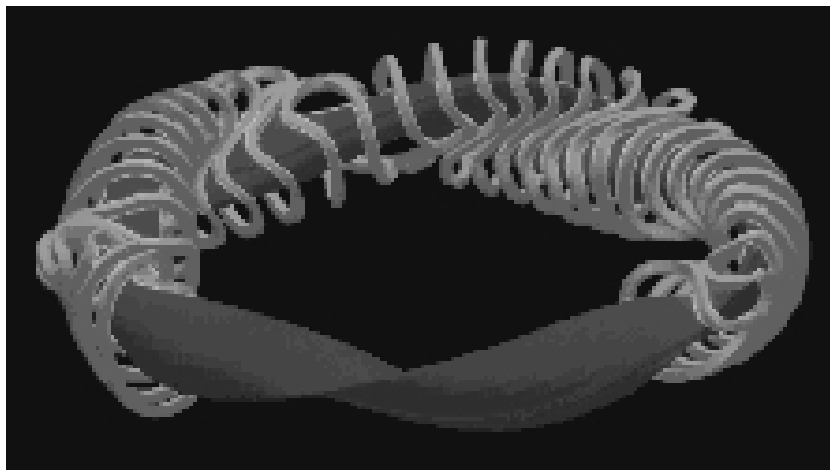

Figure 31: *Computer drawing of some modular coils and plasma of W7-X. The five toroidal field periods will maintain the plasma such that it is bean shaped at the corners of the pentagon [2, 1].*

The main purpose of W7-X is to yield convincing proof of the reactor properties of stellarators. Because the plasma properties of tokamaks are likely to be extended to stellarators the W7-X will use deuterium as fuel and thus avoid the radioactive and expensive tritium fuel [1].

Essential data of the W7-X fusion experiment is given below [1]:

```
Total diameter                          15 m
Height                                  approx.  4 m
Mass                                    550 000 kg
Major plasma radius                     5.5 m
Mean minor plasma radius                0.53 m
Magnetic field                          3 T
```

D.2.1   Planned neutron diagnostics

In addition to the BF_3-counters and fission chambers treated in this report a number of neutron diagnostic systems for W7-X are proposed such as:

- ^{3}He Bonner spheres measuring the time resolved total neutron emission rate.

- An activation system measuring time integrated total neutron yield.

- A time-of-flight spectrometer measuring neutron energy spectra.

A long term plan of the neutron diagnostics for W7-X is presented in [3].

References

[1] WENDELSTEIN 7-X Fusion Experiment,
http://www.ipp.mpg.de/ipp/w7x.eng.html, Max-Planck-Institut
für Plasmaphysik, Public Relations Office, Garching bei München.

[2] F. Wagner, The W7-X Stellarator Project, Europhys. News **26**
(1995).

[3] T. Elevant, B. Wolle, A. Weller, Neutron Diagnostics for W7-X:
A Long Term Plan for the Period 1996-2005, IPPIII/217, Jan-
uary 1997, Max-Planck-Institut für Plasmaphysik, Garching bei
München.

[4] Judith F. Briesmeister, Editor, MCNP-A General Monte Carlo N-
Particle Transport Code, version 4B, LA-12625-M, March 1997, Los
Alamos National Laboratory.

[5] The WENDELSTEIN 7-AS Fusion Experiment,
http://www.ipp.mpg.de/ipp/w7as.eng.html, Max-Planck-Institut
für Plasmaphysik, Public Relations Office, Garching bei München.

[6] D.J. Bennet & J.R. Thomson, The Elements of Nuclear Power, 3:rd
ed, 1989, Longman Scientific & Technical.

[7] Glenn F. Knoll, Radiation Detection and Measurement, 2:nd ed,
1989, John Wiley & Sons, Inc.

[8] Charles D. Harmon II, Robert D. Busch, Judith F. Briesmeister,
R. Arthur Forster, Criticality Calculations with MCNP: A Primer,
LA-12827-M, 1994, Los Alamos National Laboratory.

[9] Nicholas Tsoulfanidis, Measurement and Detection of Radiation,
1983, Hemisphere Publishing Corporation, McGraw-Hill Book
Company.

[10] Kenneth S. Krane, Introductory Nuclear Physics,1988, John Wiley
& Sons, Inc.